BUREAU OF RECLAMATION

Final Report No. ST-2024-21077-001

Numerical Modeling of Sediment Drawdown Flushing

Research and Development Office
Science and Technology
Research Program

U.S. Department of the Interior

October 2024

REPORT DOCUMENTATION PAGE		*Form Approved OMB No. 0704-0188*

1. REPORT DATE (DD-MM-YYYY)	2. REPORT TYPE	3. DATES COVERED *(From - To)*
10/08/2024	Research	10/01/2020-10/11/2024

4. TITLE AND SUBTITLE	5a. CONTRACT NUMBER
Numerical Modeling of Sediment Drawdown Flushing	XXXR4524KS-RR4888FARD2102101 (8)/F416A
	5b. GRANT NUMBER
	5c. PROGRAM ELEMENT NUMBER 1541 (S&T)
6. AUTHOR(S) Jianchun "Victor" Huang, PE, PhD Hydraulic Engineer	5d. PROJECT ID NUMBER (Final) Report ST-2024-21077
	5e. TASK NUMBER
	5f. WORK UNIT NUMBER

7. PERFORMING ORGANIZATION NAME(S) AND ADDRESS(ES)	8. PERFORMING ORGANIZATION REPORT NUMBER
Author's Organization Name and Full Address Sedimentation and River Hydraulics Group Technical Service Center Bureau of Reclamation	
9. SPONSORING/MONITORING AGENCY NAME(S) AND ADDRESS(ES)	10. SPONSOR/MONITOR'S ACRONYM(S)
Science and Technology Program Research and Development Office Bureau of Reclamation U.S. Department of the Interior Denver Federal Center PO Box 25007, Denver, CO 80225-0007	Reclamation 11. SPONSOR/MONITOR'S REPORT NUMBER(S) (if applicable) Report Number [XX] (2-digit number – if applicable)

12. DISTRIBUTION/AVAILABILITY STATEMENT
Final Report may be downloaded from https://www.usbr.gov/research/projects/index.html

13. SUPPLEMENTARY NOTES

14. ABSTRACT

This study employs SRH-2D to investigate the impact of reservoir geometry on drawdown flushing efficiency. The model was calibrated using data from a 2014 flushing event, reproducing observed sediment release concentrations and loads.

To examine the influence of reservoir shape, simulations were conducted with various modified geometries. Two approaches were employed: 1) altering reservoir width at different depths while maintaining constant capacity and 2) modifying reservoir width at ratios (0.5, 1, 2, 4) relative to the original width, with corresponding capacity adjustments.

Reservoir operation rules, including winter pool elevation, drawdown flushing elevation, refilling date, and summer irrigation flow rate, were incorporated into the simulations as the downstream boundary condition.

By understanding the relationship between reservoir shape and flushing efficiency, this study provides valuable insights for optimizing reservoir management and extending their operational life.

15. SUBJECT TERMS
Reservoir Sedimentation, Drawdown Flushing, Numerical Model, Reservoir Sustainability.

16. SECURITY CLASSIFICATION OF:			17. LIMITATION OF ABSTRACT	18. NUMBER OF PAGES	19a. NAME OF RESPONSIBLE PERSON
a. REPORT	b. ABSTRACT	c. THIS PAGE			Jianchun "Victor" Huang
U	U	U			19b. TELEPHONE NUMBER *(Include area code)* 303 445-2158

Mission Statements

The U.S. Department of the Interior protects and manages the Nation's natural resources and cultural heritage; provides scientific and other information about those resources; honors its trust responsibilities or special commitments to American Indians, Alaska Natives, Native Hawaiians, and affiliated Island Communities.

The mission of the Bureau of Reclamation is to manage, develop, and protect water and related resources in an environmentally and economically sound manner in the interest of the American public.

Disclaimer

Information in this report may not be used for advertising or promotional purchases. The data and findings should not be construed as an endorsement of any product or firm by the Bureau of Reclamation, Department of Interior, or Federal Government. The products evaluated in the report were evaluated for purposes specific to the Bureau of Reclamation mission. Reclamation gives no warranties or guarantees, expressed or implied, for the products evaluated in this report, including merchantability or fitness for a particular purpose.

Acknowledgements

The Science and Technology Program, Bureau of Reclamation, sponsored this research. Yong Lai and Blair Greimann provided valuable insights and discussions. Alex Greimann and Vincent Benoit assisted in designing some of the reservoir shapes. Benjamin Abban provided peer review. The Technical Communications Group assisted with proofreading and report formatting.

Cover Image – Paonia Reservoir outlet works intake structure during emergency actions to maintain diversion (Bureau of Reclamation, November 2014).

Numerical Modeling of Sediment Drawdown Flushing

Final Report No. ST-2024-21077-001

Prepared by:

Technical Service Center
Sedimentation and River Hydraulics Group
Jianchun Victor Huang, Ph.D., P.E.

Peer Review

Bureau of Reclamation
Research and Development Office
Science and Technology
Research Program

Final Report No. ST-2024-21077-001

Numerical Modeling of Sediment Drawdown Flushing

JIANCHUN HUANG

Digitally signed by JIANCHUN HUANG
Date: 2024.10.09 14:37:44 -06'00'

Prepared by: Jianchun Victor Huang, Ph.D., P.E.
Hydraulic Engineer, Sedimentation and River Hydraulics Group, 86-68240

BENJAMIN ABBAN

Digitally signed by BENJAMIN ABBAN
Date: 2024.10.09 14:56:23 -06'00'

Peer review by: Benjamin Abban, Ph.D.
Hydraulic Engineer, Sedimentation and River Hydraulics Group, 86-68240

Acronyms and Abbreviations

1D	one-dimensional
2D	two-dimensional
3D	three-dimensional
CAP	capacity of the reservoir
ft	feet
ft^3/s	cubic feet per second
g/L	grams per liter
HEC-RAS	Hydrologic Engineering Center's River Analysis System
km	kilometers
kt	kilotons
lb/ft^2	pounds per square foot
$lb/ft^2/hr$	pounds per square foot per hour
MAR	mean annual runoff
MAS	mean annual inflow of sediment
mg/L	milligrams per liter
m	meter
m^3/s	cubic meters per second
mm	millimeter
Reclamation	Bureau of Reclamation

Symbols

=	equals
>	greater than
<	less than
%	percent

Contents

Tables

Figures

1.0 Introduction

While reservoirs on natural rivers provide water for irrigation, municipal supply, power, recreation, navigation, and flood control, reservoirs increase the water surface level, reduce the flow velocity, and introduce undesired reservoir sedimentation. Reservoir silting reduces the reservoir capacity to store water, obstructs water intakes, creates flooding, impacts navigation, and alters ecology.

It has been estimated that the world wide annual reservoir storage loss rate has been between 0.5 to 1 percent (%), relative to initial installed capacity (Mahmood 1987; Annandale 2001; White 2001; Basson 2009; Wisser et al. 2013). Reservoir sustainability will require actions to either remove reservoir sediment or pass reservoir sediment through or around the reservoir. Failure to manage reservoir sediment at current stage will eventually result in dam decommissioning with substantial costs and either the loss of project benefits or increased costs of future water storage.

Reservoir sustainability solutions include: better watershed land-use practices to reduce the sediment yield entering a reservoir; sediment bypass around the reservoir through diversion channel, tunnel, or pipe; passing inflowing sediment by meanings of turbidity currents through a low-level dam outlet; sluicing of incoming sediment during partial reservoir drawdown; and flushing of sediments previously deposited in the reservoir (Shen 1999; Randle et al. 2015). Reservoir sediment removal also includes all types of dredging: mechanical, hydraulic, and hydrosuction, and their costs are usually very high.

Sediment sluicing/flushing is a cost-effective way to managing sediment in reservoirs. Sediment sluicing passes incoming sediment directly to the downstream of the dam and sediment flushing resuspends the previously deposited sediment and transports them downstream. Both methods involve opening of low-level gates in the dam to allow large outflow rate to transport sediment out of reservoirs through the intakes; thus, they are referred to as sediment flushing in this paper.

Reservoir sedimentation is impacting all Bureau of Reclamation (Reclamation) facilities. For example, the outlet works of Paonia Reservoir in Colorado became partially blocked with sediment and debris and emergency action was necessary to maintain water deliveries. A sediment flushing plan can be used to lower the reservoir pool in the early spring, and to sluice and flush sediment with high spring run-off flows through the outlet works before closing the gates to refill the pool for the irrigation season. Currently, sediment flushing is simulated by Sedimentation and River Hydraulics-One Dimension (SRH-1D), a one-dimensional (1D) cross-section based flow and sediment transport model. However, detailed sediment flushing patterns in the reservoir cannot be simulated with a 1D model because it averages all variables across a given cross section. A two-dimensional (2D) model depth-averaged model would provide more detailed sediment flushing estimates and better predict the efficiency, timing, and downstream impact of the sediment flushing.

This study is composed of four parts:

- Guidance for Reservoir Drawdown Flushing: Providing recommendations and best practices for effective reservoir drawdown flushing.
- Literature Review: A comprehensive review of one-dimensional (1D), two-dimensional (2D), and three-dimensional (3D) numerical models related to reservoir drawdown flushing.

- Calibration of a 2D Model: Calibration of a 2D model based on the spring drawdown flushing of the Paonia Reservoir in 2014.

- Comparative Analysis: A comparison of drawdown flushing processes in reservoirs with varying shapes.

2.0 Some Guidance for Reservoir Drawdown Flushing

There are two types of reservoir sediment flushes: pressure (or local) flushing and drawdown flushing. Pressure flushing opens the outlet gate(s) for a short time while maintaining reservoir pool level at a relatively high level. Drawdown flushing lowers the pool elevation creating a larger energy gradient and increased flow velocity to erode the sediments from the reservoir and to transport them downstream from the dam. The effects of pressure flushing and drawdown flushing are illustrated in figure 1, where the left two figures are for pressure flushing and the right two for drawdown flushing. For a wide reservoir, a flushing channel usually occurs during the drawdown flushing, as shown in figure 1. Figure 2 shows that the sediment outflow reduces significantly for pressure flushing as compared with drawdown flushing (Lai and Shen 1996; Shen 1999). In that figure, the vertical coordinate represents the sediment load flushed out of the reservoir, the sediment loads in the pressurized flushing cases are more than one order smaller than the sediment loads between in the two straight lines, representing two cases of drawdown flushing.

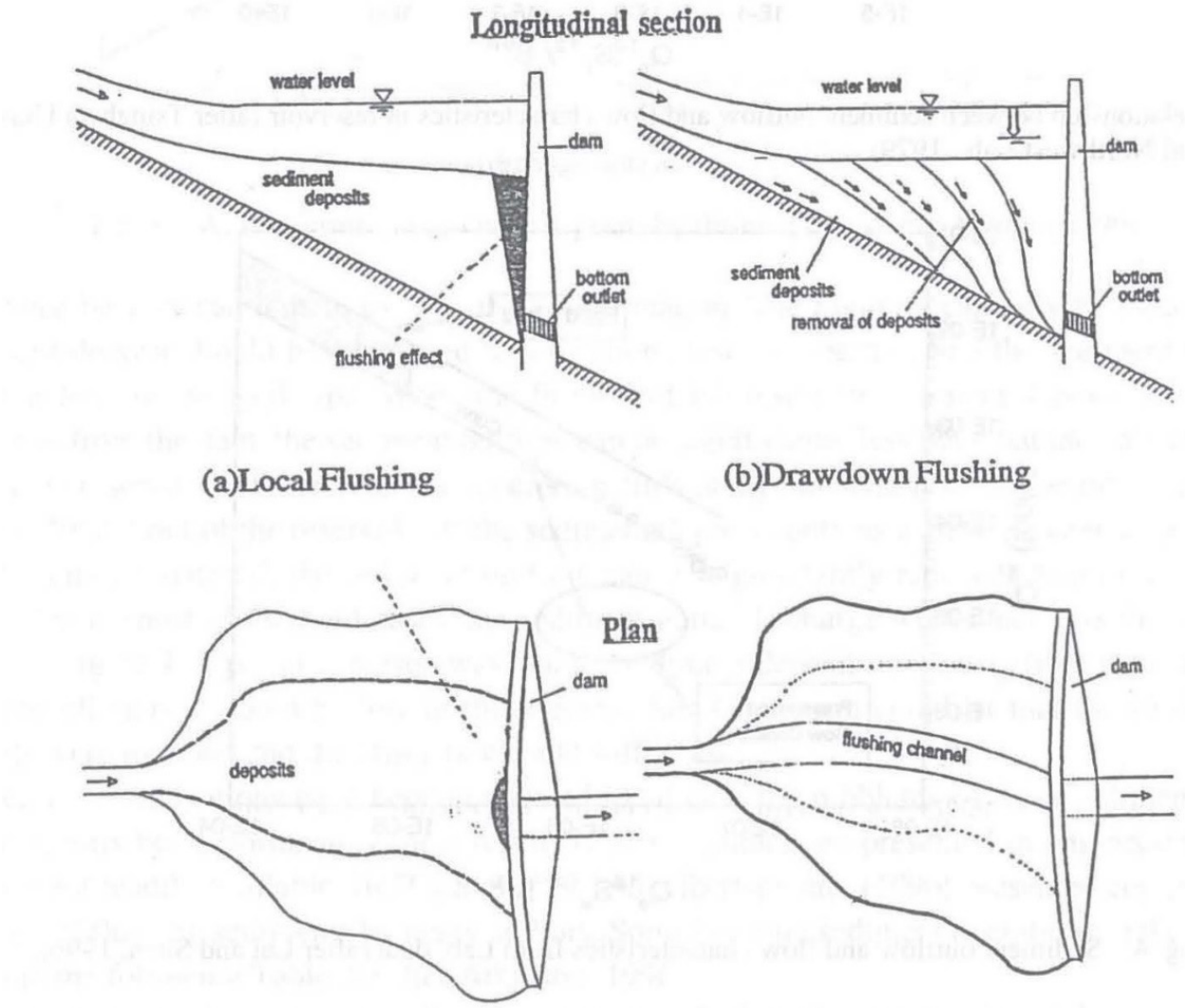

Figure 1.—Sediment erosions in pressure (local) flushing and drawdown flushing (Shen 1999).

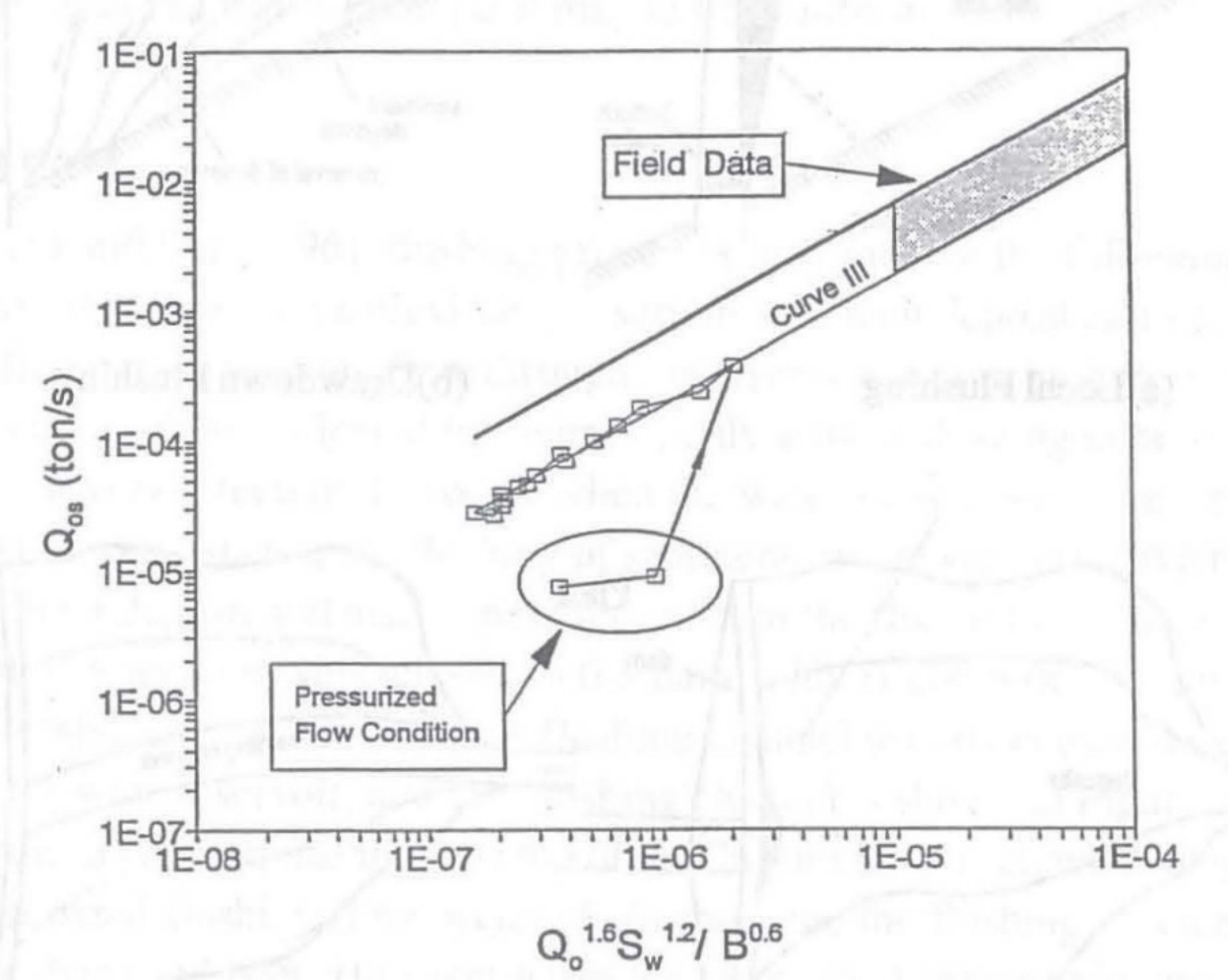

Figure 1.—Sediment outflow and flow characteristics in pressure flushing and drawdown flushing (Lai and Shen 1996; Shen 1999).

Pressure flushing is usually used in reservoirs where water storage is of value. Sediment eroded from the reservoir are usually limited to a small area immediately upstream of the gate, as shown in figure 1. Pressure flushing is usually used in large reservoirs where the water storage is of value. Pressure flushing is used to clean sediment and debris near the gate(s) and to prevent the outlet from becoming buried and clogged.

Drawdown flushing lowers the reservoir level, establishing river-like flow conditions with increased velocity, energy gradient, and sediment transport capacity. Drawdown flushing has proved to be effective in some cases. Drawdown flushing is usually effective in narrow reservoirs, however, it also involves large volumes of water passing through the dam; and it requires the reservoir to be emptied (Atkinson 1996). Drawdown flushing is not always practical and when it is poorly managed one may only move sediment from the upstream delta farther into the reservoir rather than routing it all the way past the dam (Dahl and Ramos-Villanueva 2019). Drawdown flushing can be best practiced in the following conditions: narrow valleys with steep

sides, steep longitudinal slopes, river flow above the threshold to mobilize and transport sediment, and low-level gates large enough to pass flows, and strongly seasonal flow patterns (Morris and Fan 1998;, White 1990).

Dahl and Ramos-Villanueva (2019) presented some guidance for reservoir drawdown flushing based on three factors: the total capacity of the reservoir (CAP), the mean annual runoff to the reservoir (MAR), and the mean annual inflow of sediment to the reservoir (MAS). Low ratios of CAP/MAR (<0.1) and CAP/MAS (<30) are required for a successful sediment flush (Atkinson 1996; Sumi 2008; Kondolf et al. 2014; and Dahl and Ramos-Villanueva 2019).

When drawdown flushing is used in a wide reservoir, a flushing channel occurs, as showing in figure 1, and sediment can only be resuspended in the flushing channel. According to Atkinson (1996), the flushing channel width B can be approximated by a function of the flow discharge ($B = 12.8Q_f^{0.5}$, where B is in meter and Q_f is the flushing discharge in cubic meters per second [m^3/s]). This relation can be used when the reservoir sediment has reached near the dam. This flushing channel width should be re-examined based on local conditions. Randle et al. (2015a) found that the channel width was highly variable spatially and temporally during the reservoir drawdown when the Elwha Dam and Glines Canyon Dam were removed on the Elwha River, Washington. The river channel was narrower where it came in contact with more cohesive sediment and wider where it contacted coarser and noncohesive sediment. The channel in the upstream half of the reservoir became highly braided changing course daily while reworking noncohesive coarse delta sediment.

It should be mentioned that when the incoming sediment concentration is very high and the flow contains very fine materials, the sediment-laden flow plunges beneath the clear water in the reservoir forming turbidity current. The turbidity current flows on the bed of the reservoir which can be released by reservoir outlet. The turbidity current may be able to entrain the reservoir sediments passing the outlet. Pressure flushing with turbidity current can also be an effective way to remove reservoir sediment. A turbidity current model is required to simulate this case.

Atkinson (1996) defined the sustainable reservoir capacity as the storage capacity of a reservoir which can be sustained by flushing in the long term. If the reservoir is narrower than the width of a self-formed channel produced by the flushing flow, then most of the sediment can be flushed out of the reservoir. If the flushing channel width is much narrower than the reservoir width, the sustainable reservoir capacity would be smaller than the initial storage capacity. A rough estimation was given to estimate the sustainable reservoir capacity by the final bed profile and the side slope. The final channel slope can be estimated from the initial bed profile and the difference between the dam outlet and initial bed elevation at the dam. The channel side slope can be predicted from the sediment dry density. The results should be treated with caution.

Four stages are involved in a drawdown flushing:

1. When the low-level outlets are first opened, local high velocity flow entrains the fine material deposits close to the outlet resulting in a short period of high sediment concentration outflow. This stage is similar to pressure flushing.

2. After the local deposits are removed, the velocity becomes too small even to move the fine material. This stage is similar to the final stage of pressure flushing.

3. When the reservoir level is further drawn down lower than the reservoir entrance, the sediment depositions near the reservoir entrance are entrained. At this stage, fine sediment can be carried downstream from the reservoir, coarse sediment might be redeposited in the reservoir close to the dam.

4. In the final stage, when the water stage is low and the reservoir becomes a riverine channel, the sediment previously deposited in the reservoir can be resuspended and transported downstream from the dam.

There are many flushing criteria for determining whether flushing at a particular reservoir will be successful. Some of the quantitative criteria are listed here:

1. The ratio of reservoir capacity to mean annual runoff. This value must be less than 1/50 reported by Annandale (1987). A value of 1/25 was suggested for reservoirs with a half-life shorter than 100 years by Ackers and Thompson (1987).

2. The ratio or reservoir capacity to mean annual sediment inflow sediment. This value must be less than 30 (Atkinson 1996; Sumi 2008; Kondolf et al. 2014; Dahl and Ramos-Villanueva 2019).

3. The flushing efficiency which is the ratio between the volume of sediment flushed out and the volume of water employed (Atkinson 1996).

4. The cost of operation which is the ratio between expenses of mechanical excavation and the loss of water and hydropower.

Figure 3 summarizes flushing projects from diverse environments which shows that for flushing to be successful the ratio CAP/MAR should not exceed 4% (Kondolf et al. 2014).

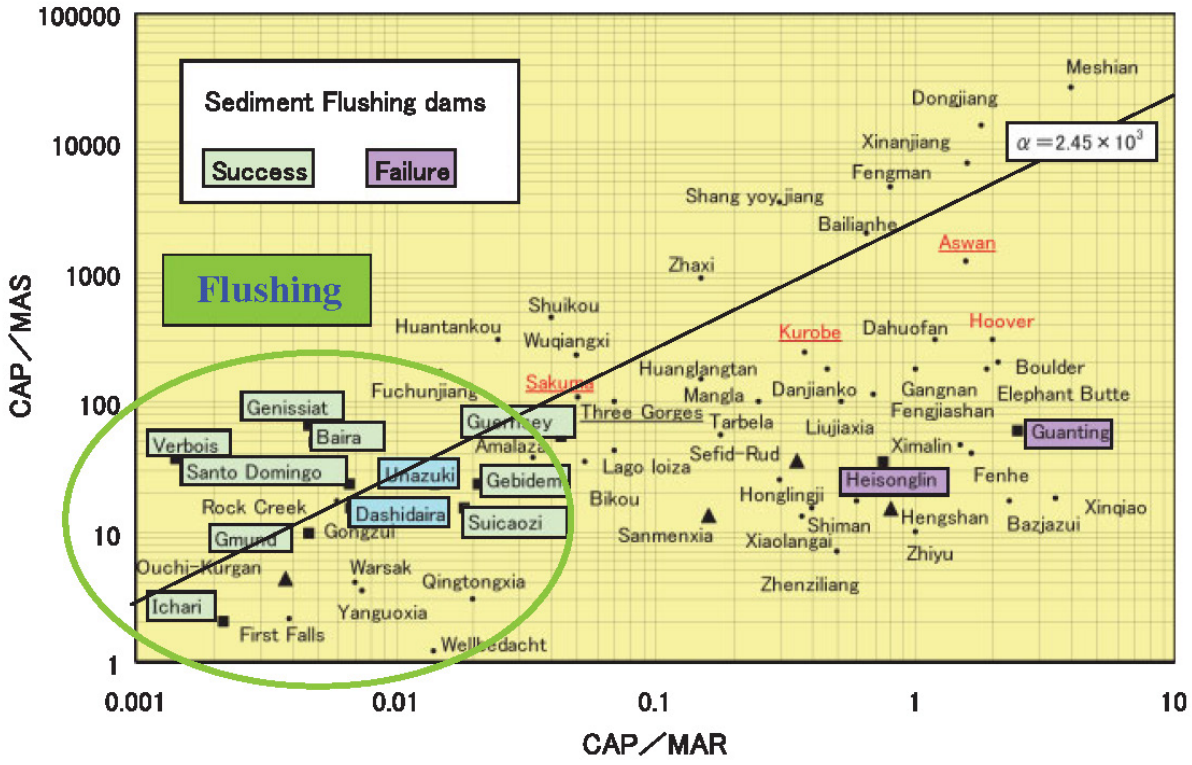

Figure 2.—Plot of flushing project with CAP/MAR and CAP/MAS (Kondolf et al. 2014).

The physical process of reservoir sediment flush depends on many factors, some of which are listed here.

1. Geometry of reservoir including the width, depth, and area-capacity table;
2. reservoir sediment particle size and sediment distribution;
3. annual flow and flow hydrographs;
4. incoming sediment load and sediment class sizes and concentration of sediment hydrography;
5. outlet opening size, elevation, and location;
6. reservoir operation rules;
7. sediment concentration constraint of reservoir release, and
8. allow or disallow sand deposition in the downstream gravel-bed channel (e.g., Chang et al. 1996).

Of the list, factors 1–6 should be known before designing a reservoir sediment flush operation and factors 7–8 should be obtained by a numerical/physical model or from sediment monitoring and in some cases are optional depending on environmental constraints. Thus factors 7–8 can also be included in the flushing criteria.

3.0 Literature Review of Numerical Modeling Studies of Reservoir Drawdown Flushing

Numerical models have been widely used to study sediment hydraulic flushing. A literature review is provided concerning all three types of models: 1D, 2D, and 3D. The literature review is only focused on drawdown flushing. Some of the literature reviews were also published in Lai et al. (2024).

3.1. One-Dimensional (1D) Numerical Models

One-dimensional numerical models offer a balance between limited empirical models and more complex and computationally expensive 2D and 3D models. The 1D models are appropriate in run-of-the-river reservoirs, where flow is highly channelized and transverse mixing is well accomplished.

Chang et al. (1996) used a 1D model, FLUVIAL-12, to evaluate the feasibility and effectiveness of sediment passing through reservoirs using drawdown flushing during floods. The model was applied to a series of reservoirs (Poe, Cresta, and Rock Creek) on the North Fork Feather River in northern California. In their case, the numerical model demonstrated that sediment could be flushed out of reservoirs and the reservoir capacity could be maintained by an extended drawdown flush operation during flood. In addition, the reservoir drawdown and sediment released can be controlled so that no sand would deposit on the gravel bed downstream from the reservoirs to endanger the fish habitat.

Morris and Hu (1992) used a 1D model (HEC-6) to simulate sediment flushing in the Loíza Reservoir in Puerto Rico. The numerical model indicted that the conversion of the reservoir from continuous high-pool operation to low-pool operation during flood periods would decrease sediment trap efficiency by 65%.

Liu et al. (2004) developed a 1D numerical model to simulate the 2001 sediment flush at two reservoirs in series: the Dashidaira reservoir and Unazuki reservoir on the Kurobe River in Japan. The model was used to compute the bed evolution, suspended sediment concentrations, and sediment flushed from or deposited in the two reservoirs.

Ahn (2012) and Ahn et al. (2013) used a 1D model (GSTAR4) to simulate sediment flushing in the Xiaolangdi Reservoir of the Yellow River and in Lewis and Clark Lake of the Missouri River.

Guertault et al. (2014) applied the 1D flow and sediment transport model, Mage-AdisTS, to simulate the 2012 sediment flush at the Genissiat Reservoir on the French Upper Rhone River. During the flushing operations, water and sediment were released in different levels in order to maintain an average concentration downstream from Genissiat below 5 grams per liter (g/L) throughout the operation. This is implemented by different gate opening combinations of hydraulic outlets located at three different levels (a bottom gate, a half depth gate, and a surface spillway). To calculate the sediment concentration released from the dam, the numerical model first calculated total sediment concentration in the reach, then transferred it into the vertical concentration profile based on the mass conservation and steady state vertical diffusion equation, then finally calculated the average concentration passing through the gate. The model reproduced the sediment concentrations at the bottom, half depth, and surface fairly well, but not the peak suspended sediment concentration in the bottom gate.

Boyd and Gibson (2016) used the 1D Hydrologic Engineering Center's River Analysis System (HEC-RAS) model to simulate the 2014 fall flush of the reservoir at Spencer Dam, 40 miles upstream of the confluence of the Niobrara River and the Missouri River. The reservoir has been flushed twice annually, in the spring and in the fall, in the last 60 years in an effort to remove sediment in the reservoir. However, no spring flush was performed in 2014 and it provided an opportunity to flush sediment deposited in the reservoir in an entire year. Cross sections were surveyed upstream of and downstream from the dam, with approximately 250 feet (ft) spacing in the reservoir. Suspended sediment and bed material samples were also collected during the flush at three locations downstream from the dam. The numerical model was calibrated with the reservoir sediment volume channel and downstream sediment concentration. The model underpredicted the delta scour by about 50% and over-predicted the peak sediment concentration downstream from the dam. The authors attributed the difference to the channel widening process which could not be simulated correctly by 1D models and anticipated that a lateral process model, such as Bank Stability and Toe Erosion Model (BSTEM), would improve the model result.

Brignoli (2017) applied SRH-1D’s unsteady flow and sediment transport modules to simulate the controlled sediment flush in Isolato and Madesimo Reservoirs in Italy for a total of 66 hours operation. Madesimo Dam on the Scalcoggia River, a tributary of Liro River, is located about 1.4 kilometers (km) upstream of the confluence of Scalcoggia and Liro rivers. Isolato Dam is located about 1.4 km upstream of the same confluence in the Liro River. Mechanical equipment was used to help remove the reservoir sediment once the reservoirs are empty. So the numerical model was mainly used to predict the sediment impact in the downstream of the two dams and downstream from the conference. Brignoli (2017) found out a satisfactory agreement between the computed and the observed depositional pattern Huang et al. (2019) updated SRH-1D to simulate a sediment sluicing and flushing plan for the Paonia reservoir, located on Muddy Creek in western Colorado. A proposed sediment sluicing and flushing plan was conceptualized to lower the reservoir pool in the early spring, and to sluice and flush sediment with high spring runoff flows through the outlet works before closing the gates to refill the pool for the irrigation season. The SRH-1D was modified to include a user-defined set of reservoir operation rules. Unsteady flow and sediment solutions within SRH-1D were used to simulate the reservoir filling and emptying process. The model was first calibrated with 3 years of field data and then used to predict short-term sediment management under different reservoir operations. The model showed

that reservoir trap efficiency strongly depends on the inflow volume. For the year 2016, the reservoir trap efficiency ranged from 20% when using the 90% inflow volume exceedance forecast to -3% (net erosion) when using the 10% exceedance forecast.

Artruc (2020) developed a numerical model to simulate the rate, magnitude, and timing of lateral erosion of Lake Aldwell on the Elwha River in Washington state under varying drawdown rate and grain size. The model calculated bank erosion due to excess shear stress on the bank and geotechnical failure due to difference between the water in the channel and the water within the bank; however, the hydraulic model was simplified as 1D steady flow at normal depth.

3.2. Two-Dimensional (2D) Numerical Models

Two-dimensional depth-averaged numerical models provide a more detailed representation of lateral hydraulic characteristics that are missed in an over-simplified 1D model. A 2D model can be used to simulate a reservoir with relatively large width-to-depth ratio in which sediment deposition and resuspension might substantially vary along a cross-section.

Olsen (1999) presented a 2D numerical model for reservoir sediment flushing. The model solves 2D depth-averaged equations for flow and 3D convection-diffusion equations for the sediment concentration with extrapolated flow field. The grid is adaptive in the vertical direction and changes according to the calculated water and bed levels. The numerical model was assessed by comparing with bathymetric cross-sections from a physical model study of the Kali Gandaki Hydropower Reservoir in Nepal.

Dewals et al. (2004) used WOLF 2D to simulate sediment flushing in an unknown reservoir in India. WOLF 2D is a free-surface flow and sediment solver using multi-block rectangular grids, developed by the Division of Applied Hydrodynamics and Hydraulic Engineering of the University of Liege in Belgium. The results showed a narrow channel generated by the flushing effect that was unable to extend to a very broad part of the reservoir width. It demonstrated the ability of the model to simulate sediment entrainment during a sediment flush, but no field data was able to validate the numerical results.

Boeriu et al. (2011) presented some case studies where 2D models were used for simulation of reservoir drawdown flushing. The 2D depth averaged flow and sediment transport modules of the Delft3D morphological software, developed by WL/Delft Hydraulics in cooperation with Delft University of Technology, were used for this purpose. The erosion flux in the model is calculated differently for cohesive and non-cohesive sediment, and the bed level is calculated using Exner equation. Case studies were used to predict sediment erosion in an unnamed reservoir in Sri Lanka, where several 5 to 10 days of flushing were simulated, and in the Koga Reservoir in Ethiopia, where 35 days of reservoir drawdown eroded sediment at the reservoir entrance and deposited some of them in the reservoir near the dam while transporting some downstream from the dam. No field data was used to validate the results.

Minami et al. (2012) applied a 2D width-averaged numerical model to simulate the coordinated sediment flushing and sluicing at Dashidaira and Unazuki dams on the Kurobe River in Japan.

The suspended sediment concentrations just downstream from both dams were calculated and compared with measurements well. The numerical model confirmed that the higher suspended sediments released from both dams during flushing operation.

Lai and Greimann (2012) applied SRH-2D to simulate a 6-month channel processe due to drawdown of Copco 1 Reservoir on the Klamath River. It was part of a much larger effort at Reclamation to support the Secretarial Determination on Klamath Dam Removal and Basin Restoration (Reclamation 2011). A total of 9 simulation runs were carried out, representing 3 hydrological scenarios (Dry-Year, Average-Year, and Wet-Year) and 3 reservoir bed erodibility conditions (Easy-Erosion, Medium-Erosion, and Hard-Erosion). The model predicted the formation of an incised channel due to reservoir drawdown. This incised channel was similar to pre-dam conditions.

Chen and Tsai (2017) developed a 2D model to estimate sediment erosion/deposition, bed evolution, and sediment flushing efficiency at the A-Gong-Dian Reservoir in southern Taiwan. The reservoir is wide, and the longest dam in Taiwan with a dam length of 2.4 km. The reservoir collects water from both Joushui River and Wanglai River. The simulated efficiency of the empty reservoir flushing was similar to that obtained from a laboratory model. The numerical model predicted sediment erosion upstream of the outlet in the Joushui river side and deposition in the Wanglai river side and they proposed a relocation of the outlet toward the upstream of the Wanglai river side to improve the flushing efficiency.

Iqbal et al. (2019) used the 2D numerical model BASEMENT, developed by the Laboratory of Hydraulics, Hydrology and Glaciology at ETH (Eidgenössische Technische Hochschule) Zurich, to simulate two sediment flushing test cases. The numerical model employs a finite volume technique to solve the 2D shallow water equations over an unstructured triangular mesh. The transition from subcritical to supercritical during the rapid sediment flushing process is handled by solving the Riemann problem at each cell interface with Godunov scheme. The model was used to simulated two sediment flushing testing cases: 1:40 physical model of the reservoir of the Gulpur Hydropower Plant which was being constructed on the Poonch river in Pakistan-administrated Kashmir and the laboratory flushing experiment by Lai and Shen (1995). The model reproduced the bed longitudinal and lateral erosions after flushing, and flushed sediment volume very well.

Chaudhary et al. (2019) used the MIKE21C to simulate the reservoir flush for the proposed reservoir on the Dibang River in east Asia. The reservoir will collect water from the Dri and Tangon River. A 1D model, MIKE 11, was used to calculate the long-term sediment distribution in the reservoir. MIKE21C, a 2D model over a curvilinear grid, was used to simulate the sediment deposition/flush of the reservoir with a constant inflow rate and an initial bathymetry obtained from the 1D model. The reservoir flushing would be carried out through the low-level spillway crest. The numerical model was used to estimate how much sediment can be flushed out with various flushing discharges and durations.

Artruc (2020) developed a 2D model to simulate the rate, magnitude, and timing of lateral erosion of Lake Aldwell on the Elwha River in Washington State under the effects of drawdown rate and grain size.

Goulart et al. (2023) applied Delft3D-FLOW's 2D model to study the modeling uncertainties of reservoir flushing simulations. They showed that parameters such as initial layer thickness, sediment transport equations, median particle size resulted in the great changes in simulated results.

3.3. Three-Dimensional (3D) Numerical Models

Three-dimensional numerical models have also been used to simulate reservoir drawdown flushing. With the cost of computation, 3D models are only limited to simple cases with a very short period.

Ghoreishi and Tabatabai (2010) used a 3D hydrodynamic model to simulate the reservoir sediment flushing experiments by Lai and Shen (1995). The experiments were conducted in a rectangular flume with dimensions 50 meters (m) long, 2.44 m wide, and 1.52 m high with sediment paved in a 9 m reach upstream from the dam. The numerical model predicted the channel erosion near the dam fairly well, however it did not reproduce the observed eroded channel developed longitudinally upstream. The authors attributed the deviation to the limitation of the 3D model that treated the water surface as a rigid lid. The 3D model reproduced the erosion patten in the first stage of the sediment flush (mainly pressure flushing) and showed differences in the second stage (drawdown flushing).

Esmaeili et al. (2015) employed a full 3D numerical model to simulate the 2012 sediment flushing operation in Dashidaira Reservoir in Japan. Sediment flushing operations have been performed through the bottom outlets every year during the first major flood event in the rainy season since 1991. The finite volume approach was employed using an unstructured and adaptive grid which moved vertically with changes in the bed and the free-water surface. The model was first calibrated to reduce the difference between computed and measured total volume of flushed out sediment. The simulated reservoir bathymetry after flushing operation was then compared with the measured one. The results showed that the 3D model can properly simulate the flushing channel evolutionary pattern. The numerical model also found that smaller size sediment tend to be eroded and flushed out earlier than larger sediment sizes and coarser sediment is mainly flushed out at the end of the preliminary drawdown and during the free-flow state. Esmaeili et al. (2017) presented additional calculations based on the same model, such as additional artificial discharge during the free-flow state, increasing the drawdown speed, and the construction of an auxiliary longitudinal channel.

Haun and Olsen (2012) applied the 3D model, SSIIM 2, to predict the reservoir sediment flushing process. The numerical model uses structured multiblock grid in the horizontal directions and adaptive grid in vertical directions where in the number of vertical cells depends on the water depth. Only one cell is spanning the water depth in shallow areas and a 2D calculation is done and up to 11 cells are generated in deep areas. The numerical model was applied to a physical model study of the Kali Gandaki hydropower reservoir in Nepal to reproduce the sediment volume flushed out and the bed deformation in six cross-sections. The numerical model improved the channel erosion in a bend due to the secondary currents which could not be simulated with traditional 2D model. Olsen and Haun (2018) updated the 3D model

SSIIM to include a bank failure algorithm to find the location and the depth of the slides during reservoir flushing. The domain is divided into water, soil, and slide cells. The soil domain uses a 2D depth-averaged grid and the water grid and the slide grid are both 3D. The bank failure algorithm was tested with the 2014 reservoir sediment flush on the Bodendorf Reservoir in Austria. The numerical model reproduced the number and magnitude of the slides well, but the locations were not always correct. The updated algorithms worked well for thick sediment layers, but instabilities occurred for thin layers. The numerical model SSIIM was also used by Saam et al. (2019) to simulated the efficiency of flush of the Schwarzenbach Reservoir in the Black Forest, Germany, with partial and full drawdown.

4.0 Two-Dimensional (2D) Numerical Modeling of Sediment Flushing During Paonia Reservoir Drawdown Flushing, March–October 2014

The Sedimentation and River Hydraulics – Two Dimension (SRH-2D) (Lai Y.G. 2020) was calibrated using sediment concentration measurements from 2014. Reservoir sediment release concentration data was available from March 28 to November 6, 2014. This study initiated the numerical simulation calibration on January 1, 2014, but compared the results to survey data starting on March 28, 2014.

The bed material data as Kimbrel (2015) were used in this study. Two different sources of bed material gradation data, one set from Muddy Creek and the other set from Paonia Reservoir, were used. These data are simplified into four size classes as shown table 1.

Table 1.—Bed material gradations used in the model

Class	Low limit (mm)	Upper limit (mm)	Gradations (%)	
			Delta	Reservoir
Clay and silt	0.00002	0.0625	1.0	60.0
Fine and medium sand	0.0625	0.5	76.8	31.0
Coarse sand	0.5	2	17.3	7.0
Gravel	2	16	4.9	2.0

Parameters for particle fall velocity as a function of sediment concentration are presented in table 2. Parameters for critical surface erosion shear stress, surface erosion rate, critical mass erosion shear stress, mass erosion rate, and critical partial/full deposition shear stress are listed in table 3.

Table 2.—Paonia SRH-2D sediment model fall velocity relationship

Fall velocity (mm/s)	Concentration (mg/L)
0.08	100
1.6	1,000
12.0	6,000
0.16	100,000

Table 3.—Paonia SRH-2D model parameters of critical erosion and deposition for cohesive sediment transport

Parameter	Value
Critical surface erosion shear stress (lb/ft^2)	0.2
Surface erosion rate (lb/ft^2/hr)	0.655
Critical mass erosion shear stress (lb/ft^2)	1.02
Mass erosion rate (lb/ft^2/hr)	0.655
Critical shear stress, full deposition (lb/ft^2)	0.1
Critical shear stress, partial deposition (lb/ft^2)	0. 1

A reasonable match between the modeled and observed sediment load exiting the reservoir in 2014 is shown in figure 4. This comparison spans March 28 to November 6, 2014, the period for which sediment load data is available. Sediment load was calculated from the available sediment release concentration. A notable discrepancy is the sharp increase in surveyed sediment load after November 2, which might be from a measurement error. Overall, the modeled sediment load is calibrated to be greater than the measured in most of the day until the last day.

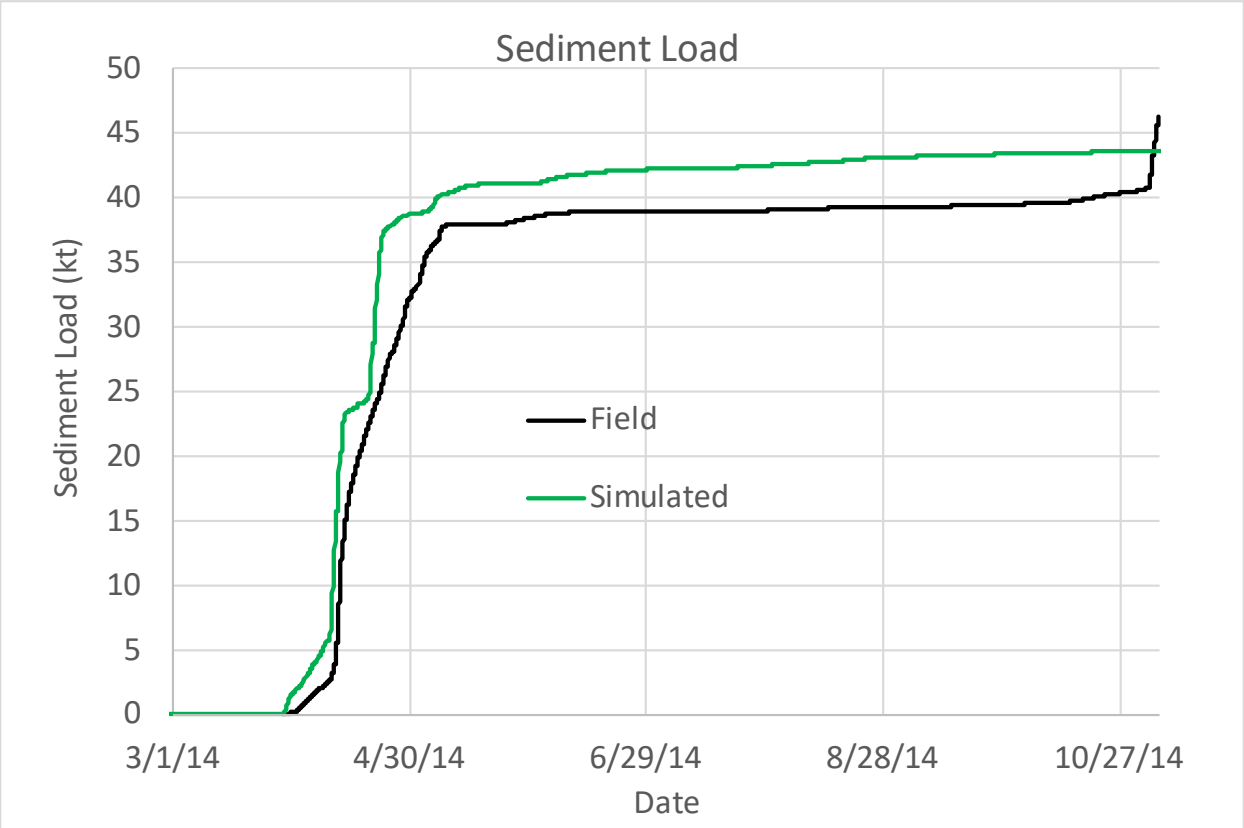

Figure 4.—Comparison of simulated and measured sediment loads in reservoir release.

Figure 5 presents the sediment load for each size fraction: fine (<0.0625 millimeter [mm]), fine sand (0.0625 mm to 0.5 mm), coarse sand (0.5 mm to 2 mm), and gravel (2 mm to16 mm). The results indicate that nearly 99.9% of the released sediment was fine, with only 0.1% being fine sand. Less than one ton of coarse sand and gravel were released.

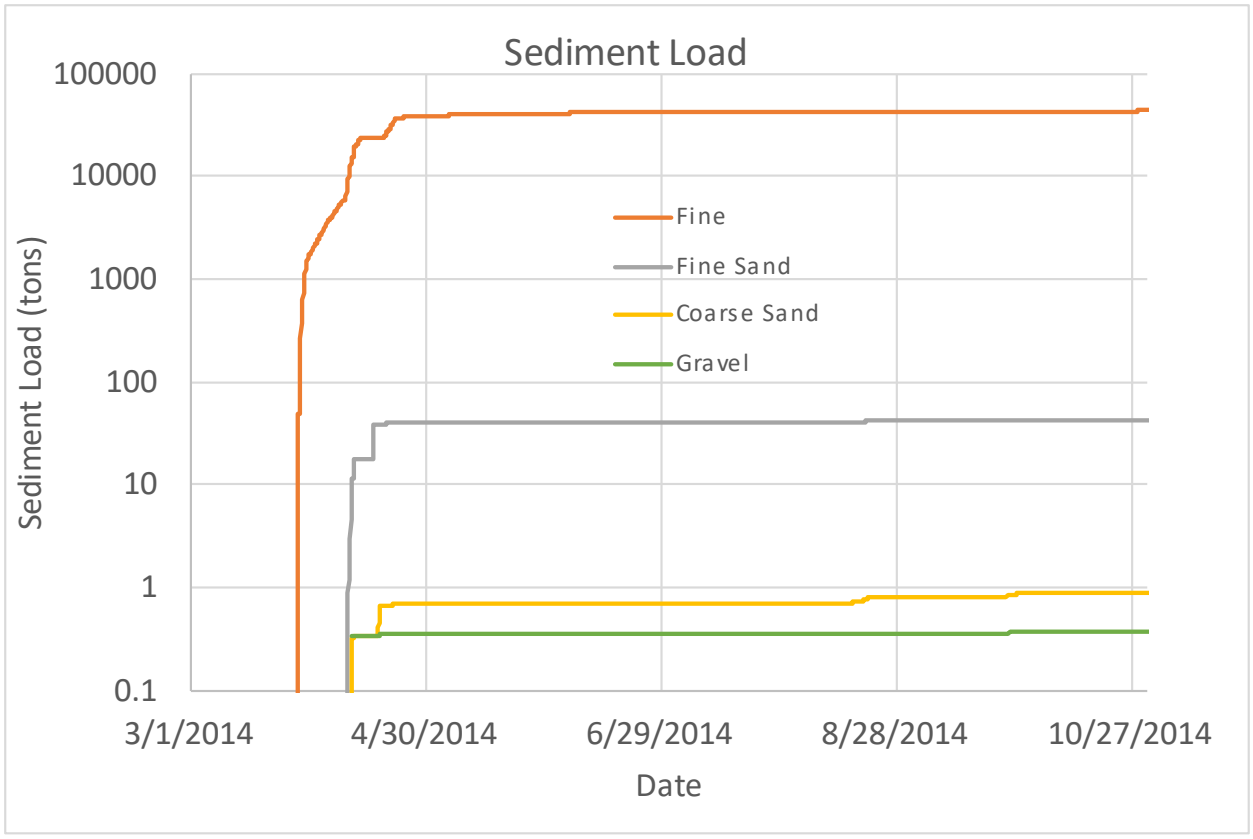

Figure 5.—Simulated sediment load in each sediment class.

The predicted outgoing suspended sediment concentration (figure 6) aligns well with observations during periods of high concentration (greater than 100 milligrams per liter [mg/L]). However, model performance is less accurate at lower sediment concentrations. Prioritization was given to matching higher concentrations, which represent the majority of sediment flux out of the reservoir. For context, the figure also displays the reservoir's incoming sediment concentration. The maximum suspended sediment concentration in the reservoir release (approximately 13,000 mg/L) is lower than the maximum incoming sediment concentration (19,000 mg/L).

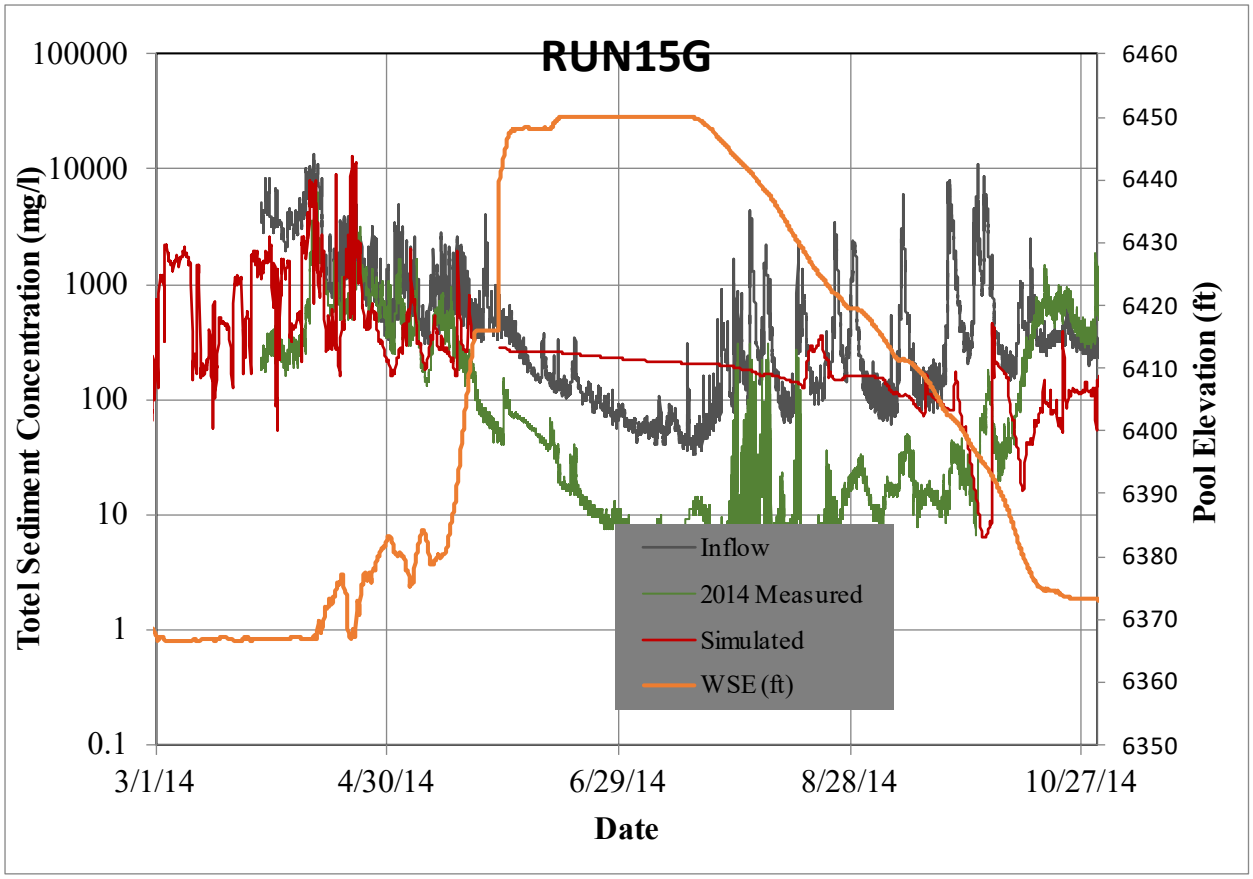

Figure 6.—Comparison of simulated and measured sediment concentrations in reservoir release.

Figure 7 illustrates the predicted erosion and deposition patterns within the reservoir following the entire simulation. While no field data is available for comparison, the model suggests erosion in the reservoir's upstream section and deposition near the dam, with most sediment flushed out during the drawdown.

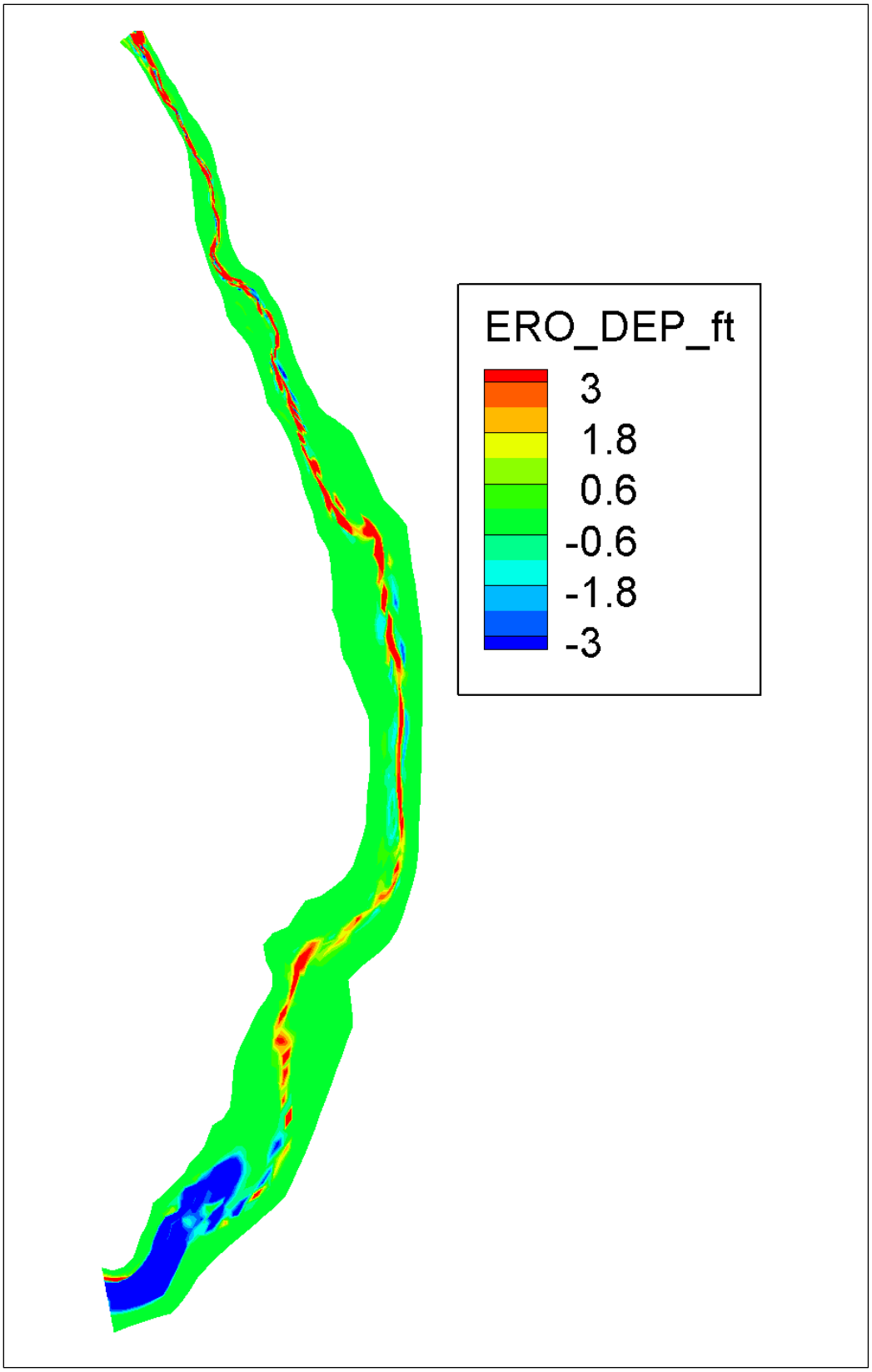

Figure 7.—Simulated erosion (red) and deposition (blue) patterns in the reservoir.

5.0 Two-Dimensional (2D) Numerical Modeling of Different Types of Reservoirs Based on Paonia Reservoir

Borland and Miller (1960) established a link between reservoir sediment distribution and reservoir shape. They categorized reservoir types by plotting depth against initial reservoir capacity on a log-log graph. The slope of the resulting line(s) determined the reservoir type. Four reservoir types were identified: Type I (lake), Type II (floodplain-foothill), Type III (hill), and Type IV (gorge). Sediment is expected to accumulate near the reservoir entrance in Type I and near the dam in Type IV.

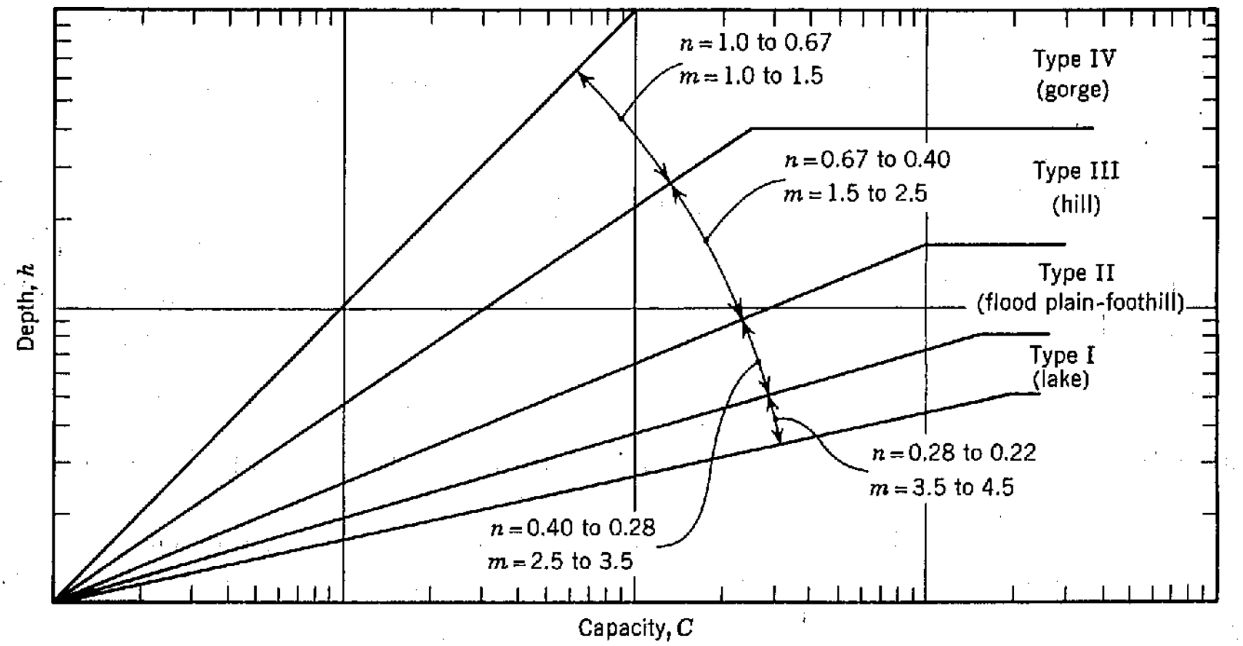

Figure 8.—Classification of reservoirs by the depth versus capacity relationship (Borland and Miller 1960).

When multiple slopes occur in the depth-capacity relationship, the slope at the higher elevation (reservoir entrance/delta) typically defines the reservoir, as the delta captures most incoming sediment. Applying this method to the Paonia Reservoir (figure 9) indicates it most resembles a Type III, floodplain-foothill reservoir.

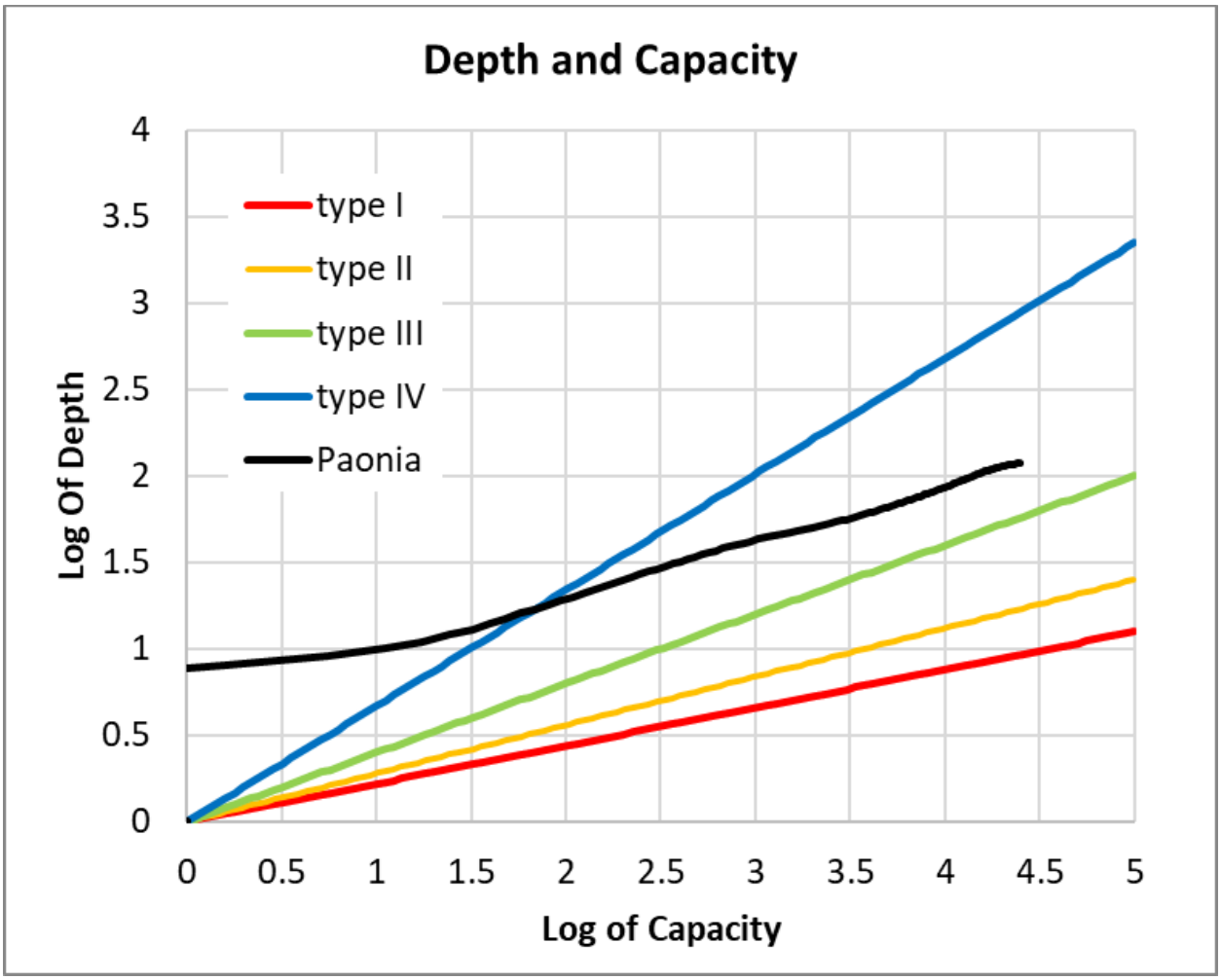

Figure 9.—Classification of Paonia Reservoir type.

To construct different reservoir types with identical normal depth, two approaches were considered. First, reservoir capacity could be adjusted to create varying widths (addressed in the next chapter). Alternatively, the capacity could remain fixed while fitting the reservoir type solely to the lower elevation near the dam, given the importance of reservoir type at lower elevations during drawdown flushing. Depth-capacity figures are presented in figure 10 and figure 11.

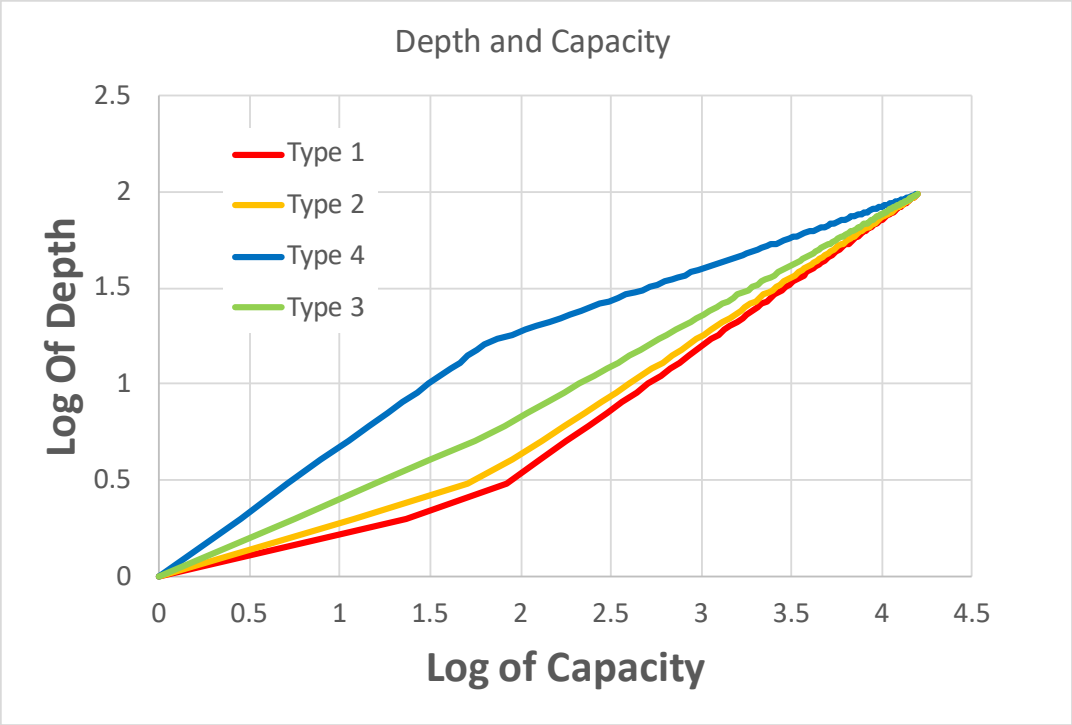

Figure 10.—Depth versus capacity relationship in log-log figure for created reservoirs based on Paonia.

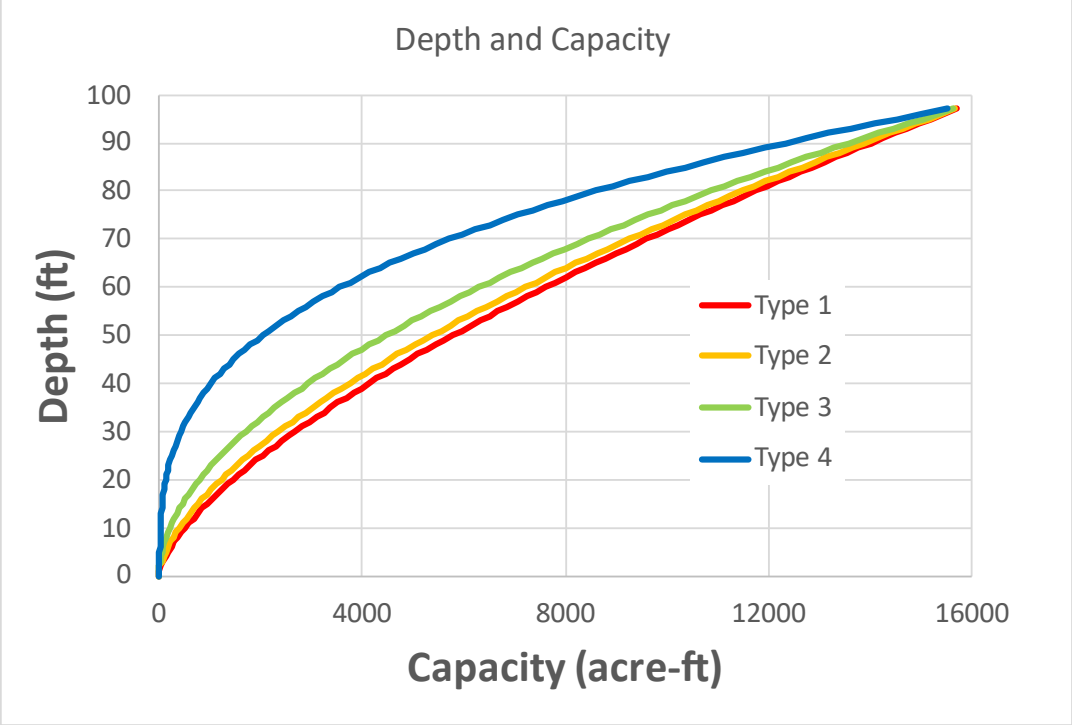

Figure 11.—Depth versus capacity relationship for created reservoirs based on Paonia.

The constructed four reservoir types share the same bed profiles as Paonia Reservoir, with a fixed 30-foot upstream channel width and a downstream channel width varying based on reservoir area. A transition zone connects these channels, gradually increasing in width. The reservoir depth versus area was derived from the depth versus capacity relationship presented in figure 10 and figure 11. Once depth-area was determined, the upstream location was calculated at a given depth from the bed profile. If the depth was small and the upstream location was downstream from the transition zone, the downstream channel width was calculated directly from the reservoir area (figure 12). If the upstream channel location was in or upstream of the transition zone at a given depth, the reservoir area included the downstream area, transition zone, and potentially the upstream area. The downstream channel width was then calculated from the total area derived from the depth-capacity table.

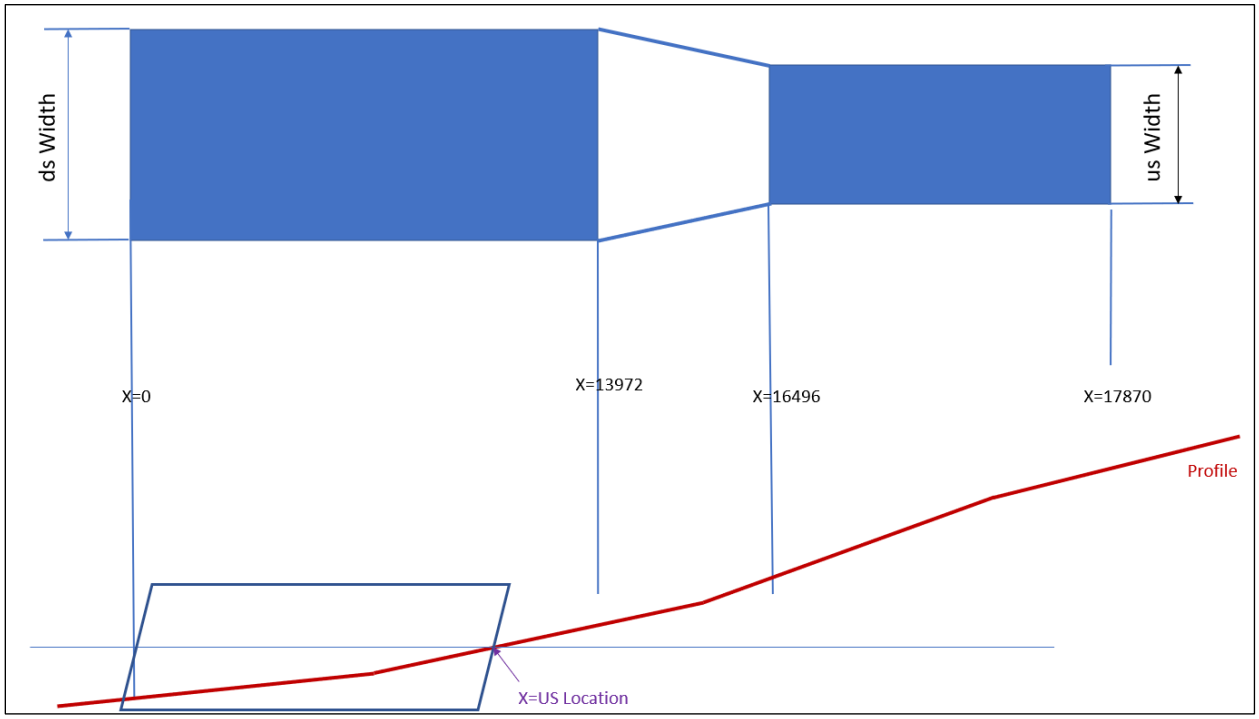

Figure 12.—Calculation of downstream channel width given channel upstream location and reservoir area.

After determining the upstream channel location and downstream channel width, a contour line was drawn. Figure 13 presents an example contour map (reservoir Type III) with contour lines at specific elevations. This contour map was projected onto the centerline of Paonia Reservoir (figure 14) and input into ArcGIS® to create the reservoir bathymetric surface.

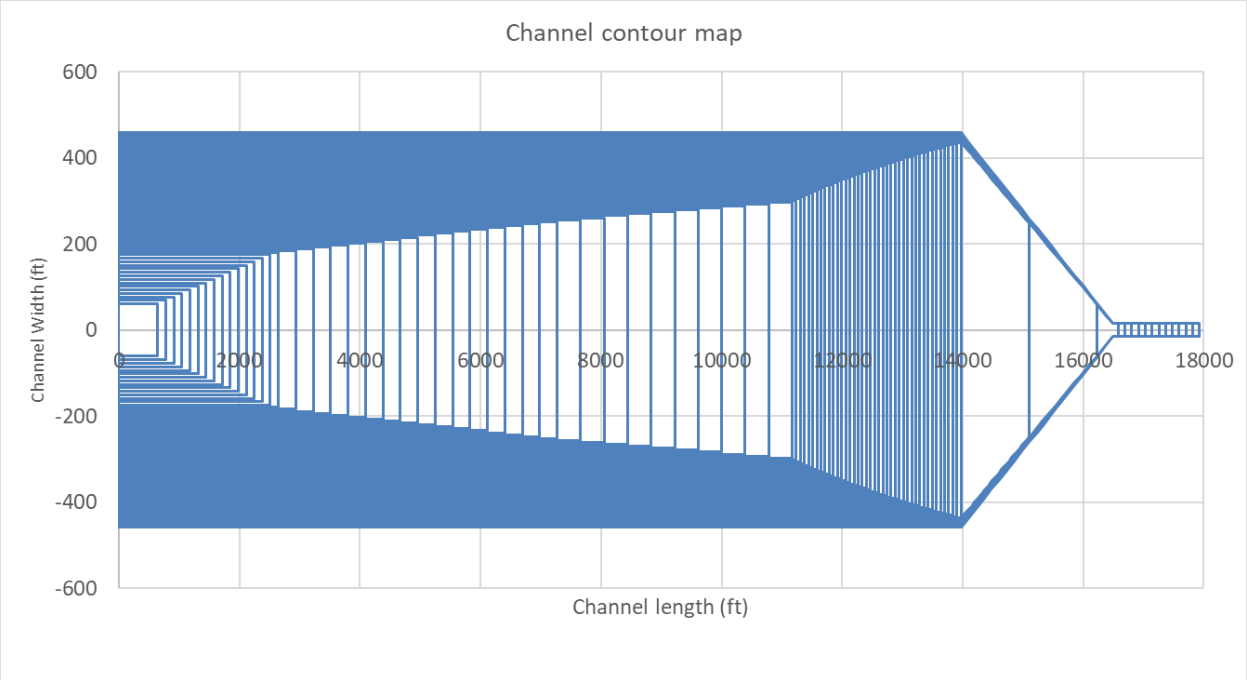

Figure 13.—Contour map of reservoir Type III in Cartesian coordinate system.

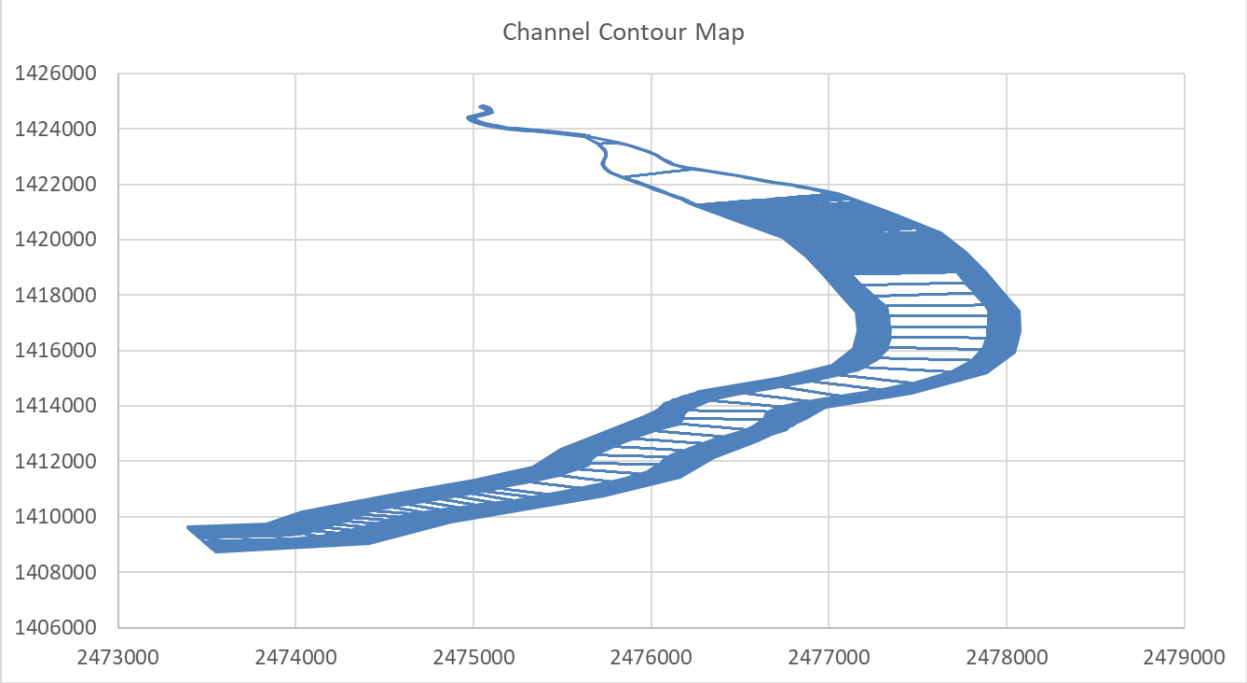

Figure 14.—Contour maps of reservoir Type III in curvilinear coordinate system.

Figure 15 displays cross-sections of the four created visual reservoirs at the dam's surface. Type I has the widest channel, and Type IV has the narrowest channel at the reservoir bottom.

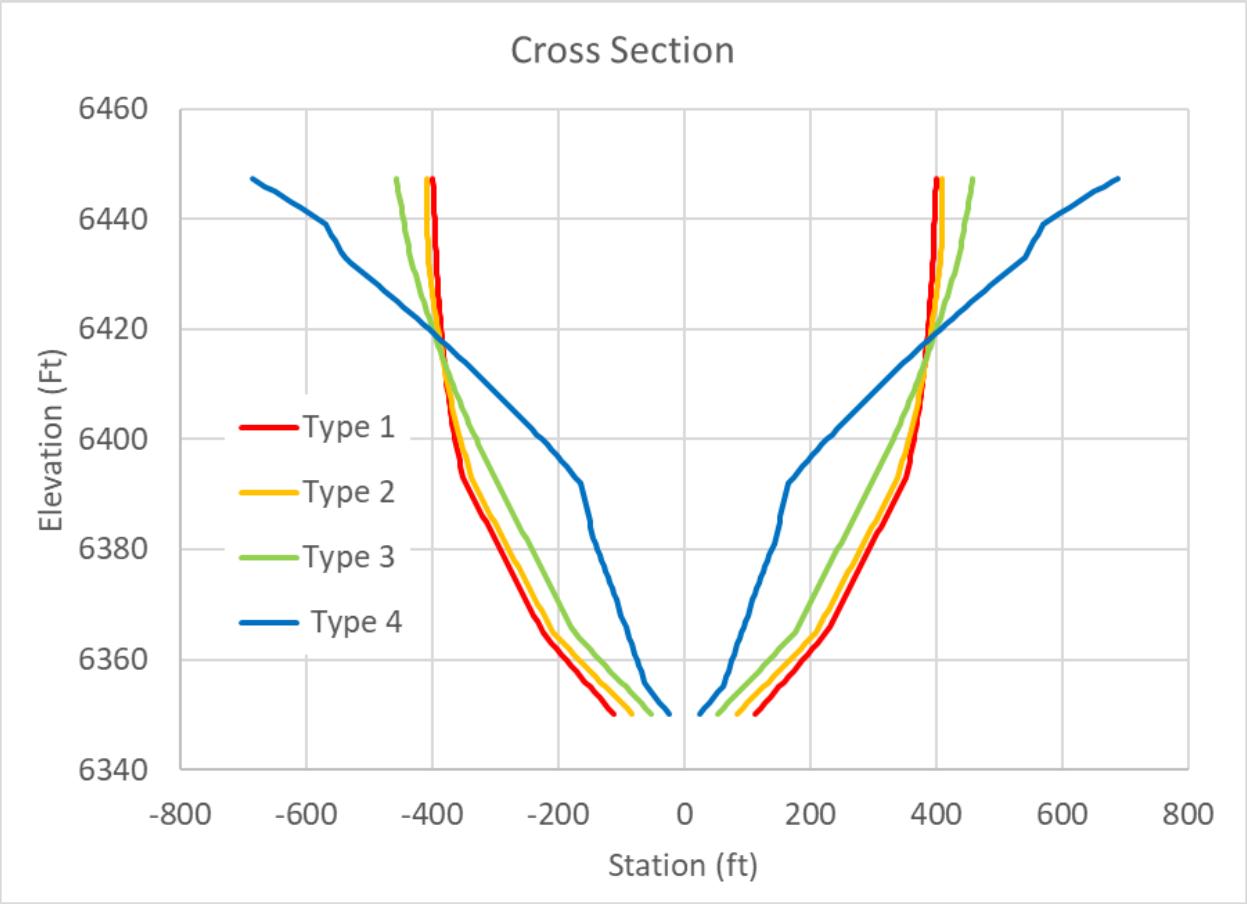

Figure 15.—Cross sections of four reservoir types at dam surface.

Numerical simulations were conducted using historical incoming flow in 2014 flow rates, sedimentation loads, and reservoir operation rules to investigate the influence of reservoir shape on the effectiveness of drawdown flushing. For this study, the drawdown flushing process was concluded on May 11.

The reservoir rules used in the study were as follows:

1. **Winter Pool:** Maintain a pool elevation of 6377 ft until February 1.

2. **Drawdown:** Reduce the reservoir level at a rate of one foot per day until reaching 6359 ft, preparing for the spring flushing.

3. **Spring Flushing:** Maintain a pool elevation of 6359 ft during the spring flushing period.

4. **Refilling:** Refill the reservoir starting on May 11.

5. **Summer Irrigation:** Release 200 ft^3/s for summer irrigation starting on August 1.

6. **Release Ramping:** Limit the reservoir release ramping rate to a maximum of 100 ft^3/s per hour.

7. **Release Capacity:** Limit the reservoir release rate at a given pool elevation to a value between the spillway capacity and the combined capacity of the outlet works and spillway.

Figure 16 presents the reservoir pool elevation as the downstream boundary condition. The reservoir level was lowered from February 1, reaching a minimum elevation of 6359 ft on February 18, in preparation for spring flushing. Spring flushing was generally effective when spring flows exceeded 350 ft^3/s. During the drawdown flushing period (April 7 to May 11), some spikes in reservoir pool elevations may have occurred due to limitations in the outlet works, which restricted flow release capacity.

In this simulation, the drawdown flushing ended on May 11, when the reservoir began refilling to store water for summer irrigation. Given that all four reservoir types have similar capacities, all reservoirs reached their normal pool elevation of 6447.5 ft within approximately 17 days of refilling.

The summer irrigation season commenced on August 1, during which a constant outflow of 200 ft^3/s was maintained until the reservoir was empty.

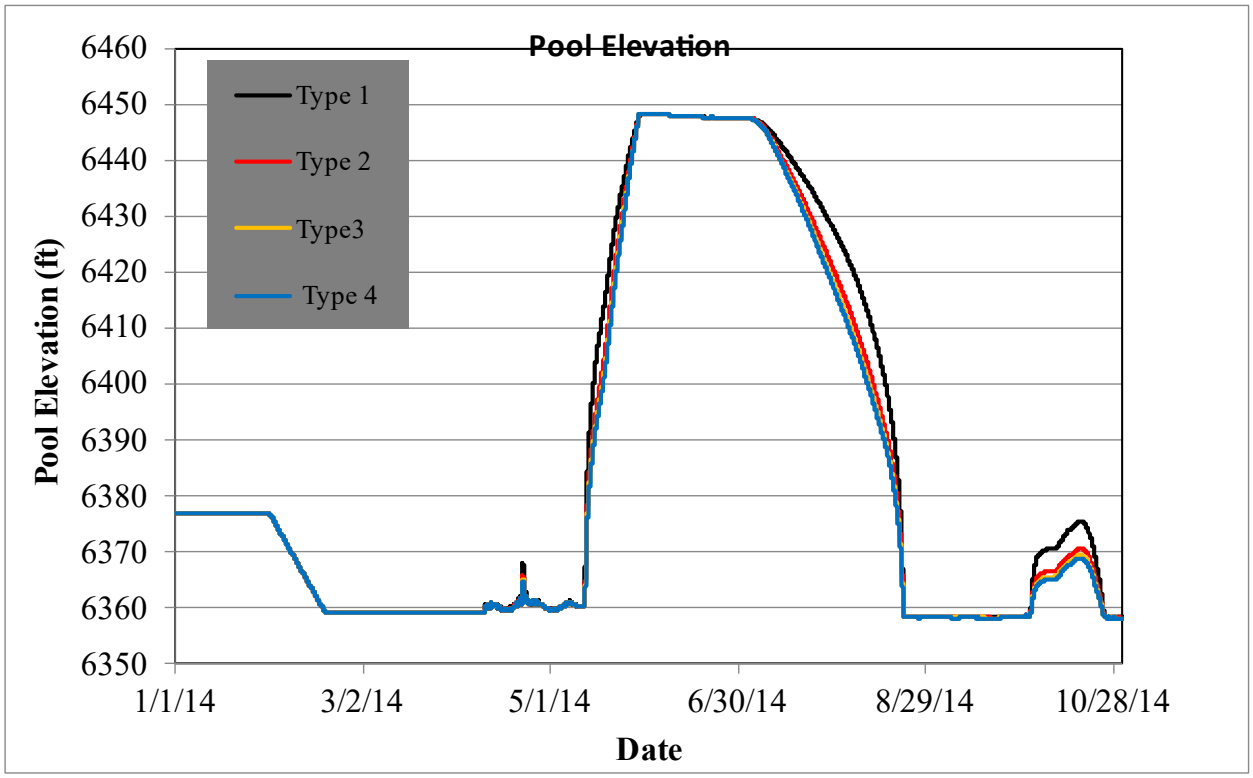

Figure 16.—Reservoir pool elevations with different reservoir types.

Figure 17 presents the simulated reservoir outflows from the 2D model. For comparison, the incoming flow is also shown. The reservoir release rates generally followed the incoming flow, except during peak flows when the outlet works could not accommodate all incoming flows. Outflow differences occurred primarily during the refilling period and afterward. The reason for these differences is uncertain and may be attributed to discrepancies between the pre-calculated and model-calculated reservoir storage. Incorporating reservoir operation rules into the model could help to directly calculate reservoir outflows within the model, using them as a downstream boundary condition instead of a predetermined water surface elevation. However, during the reservoir refilling period, both outflow and sediment release were low, minimizing the impact of errors on calculating sediment flushing efficiency.

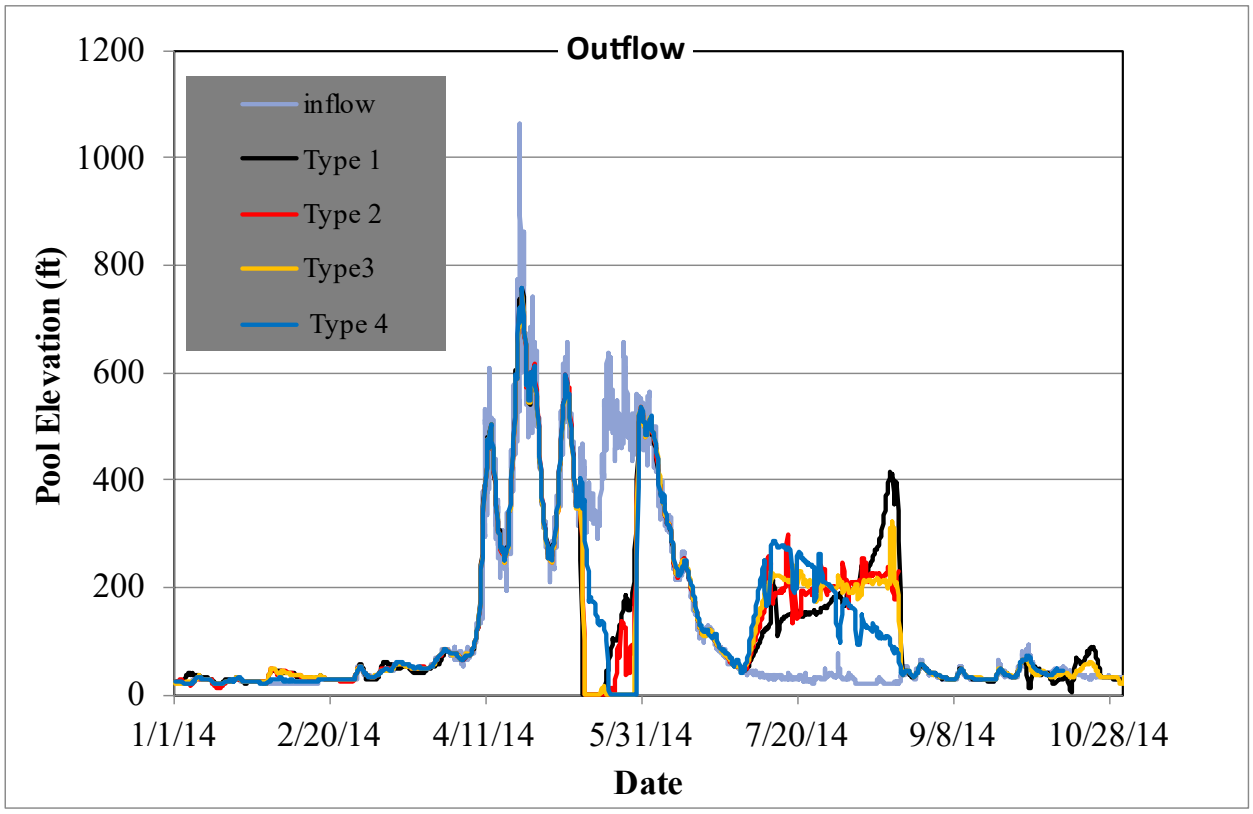

Figure 17.—Simulated reservoir outflow rates with different reservoir types.

Figure 18 shows the reservoir release concentrations during spring flushing. The numerical model indicates that Type I reservoirs had the lowest release concentrations, while Type IV reservoirs had the highest. Although all reservoirs have the same capacity, Type I reservoirs have a wider bottom, and Type IV reservoirs have a narrower bottom. Sediment concentrations were generally low before spring floods (<350 ft^3/s) and high afterward (>350 ft^3/s). However, Type IV reservoirs exhibited relatively high concentrations even before spring floods, suggesting that narrow reservoirs near the bottom can effectively flush sediment during low flows.

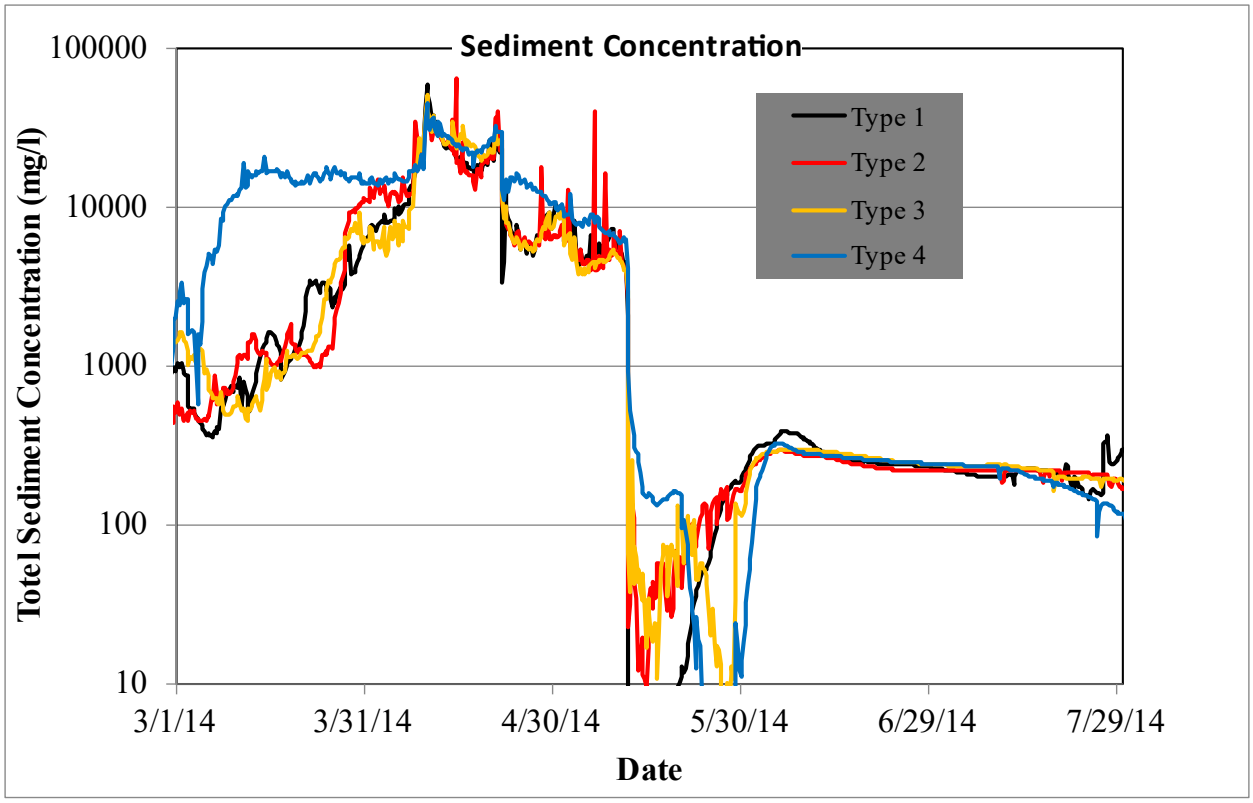

Figure 18.—Simulated reservoir release concentrations with different reservoir types.

Figure 19 presents the reservoir release loads during spring flushing. The numerical model reveals that Type I reservoirs had the lowest release loads, while Type IV reservoirs had the highest. The model demonstrates that, for the same reservoir capacity, a narrow reservoir at the bottom (Type IV) is more efficient in flushing out reservoir sediment. The unexpected finding that Type II reservoirs could flush more sediment than Type III may warrant further investigation. Type I and Type III reservoirs exhibited similar flushing performance, indicating that beyond certain limits, a wider reservoir may achieve comparable flushing efficiency to a narrower one. For all reservoir types, the flushed sediment was lower than the incoming sediment loads, emphasizing the continued dominance of reservoir capacity in flushing effectiveness.

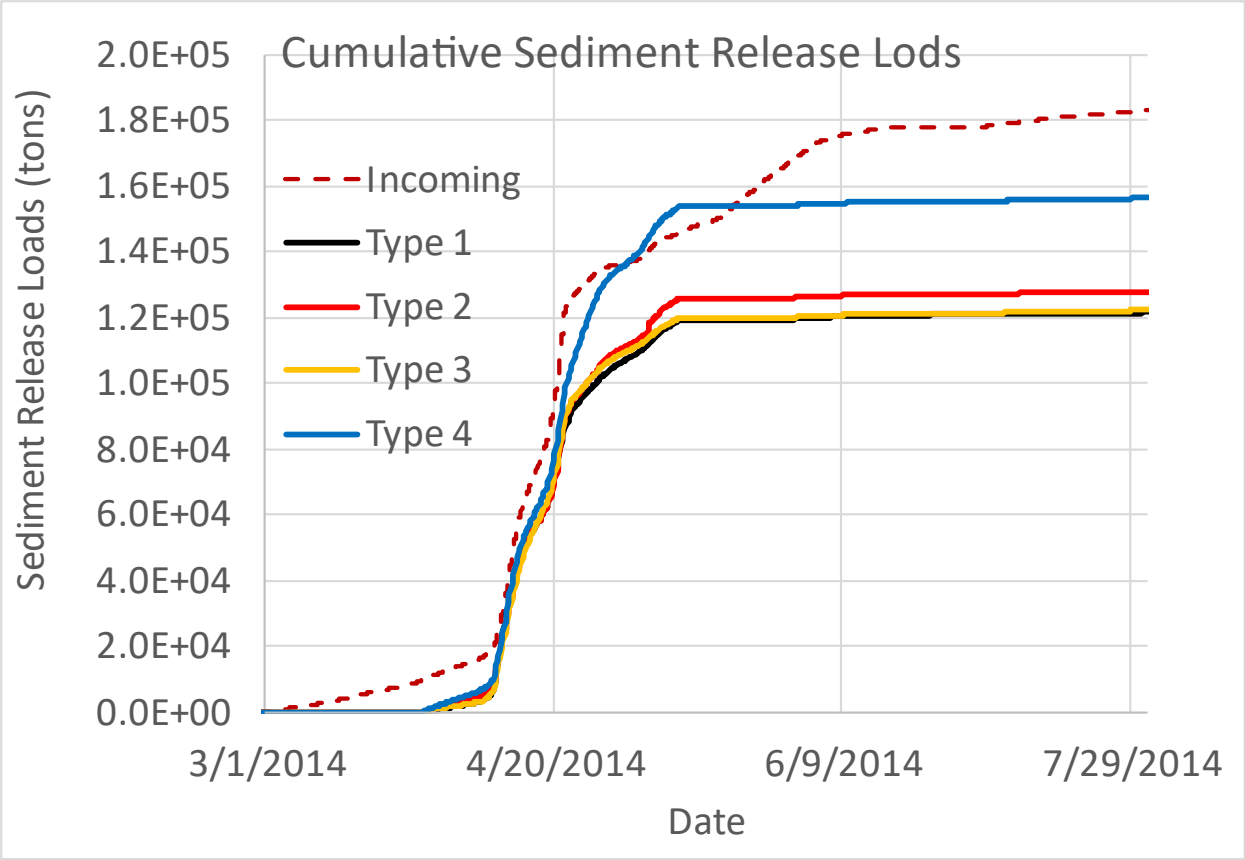

Figure 19.—Simulated reservoir release loads with different reservoir types.

Table 4 summarizes incoming sediment loads, the release loads, and sediment trapping coefficients for different types of reservoirs with the same capacity. The trapping coefficients, which measure the percentage of sediment retained in the reservoir, range from 15% in a Type IV reservoir with a very narrow reservoir bottom to 34% in a Type I with a wider bottom.

Table 4.—Sediment release loads and reservoir sediment trapping coefficients with different types of reservoirs

Incoming Load (kt)*	**183**			
Reservoir type	Type I	Type II	Type III	Type IV
Release load (kt)	122	128	122	156
Trapping coefficient	34%	30%	33%	15%

*kt: thousands of English tons

6.0 Two-Dimensional (2D) Numerical Modeling of Different Capacities of Reservoir Based on Paonia Reservoir

In this section, the width of the Paonia Reservoir was modified to investigate how the reservoir's shape affects its drawdown flushing efficiency. The new reservoir widths are 0.5, 1, 2, and 4 times the original width, while maintaining proportional changes in capacity and surface area.

To adjust the width, the original reservoir survey points were projected onto the channel centerline. For each point, its streamwise coordinate was calculated (distance along the centerline) and its transversal coordinate (distance from the centerline). Then the transversal coordinate was modified to create the new reservoir shape. Through experimentation, it was found that gradually changing the width could achieve a smoother reservoir surface.

To double the channel width, the transversal coordinate was modified by a factor of 2 squared to determine the new point's location. Then this new point was projected onto the channel's centerline and repeated the process, modifying the transversal coordinate by another factor of 2 squared. The same procedure was followed to create a reservoir width four times the original, starting with the surface that was already twice the original width.

To reduce the channel width, a single width adjustment was enough.

Figure 20 and figure 21 illustrate the updated reservoir capacity and area versus depth relationships for the various widths. The new capacity and area are propositional to the width adjustment ratio to be 0.5, 1, 2, and 4 times of original Paonia Reservoir.

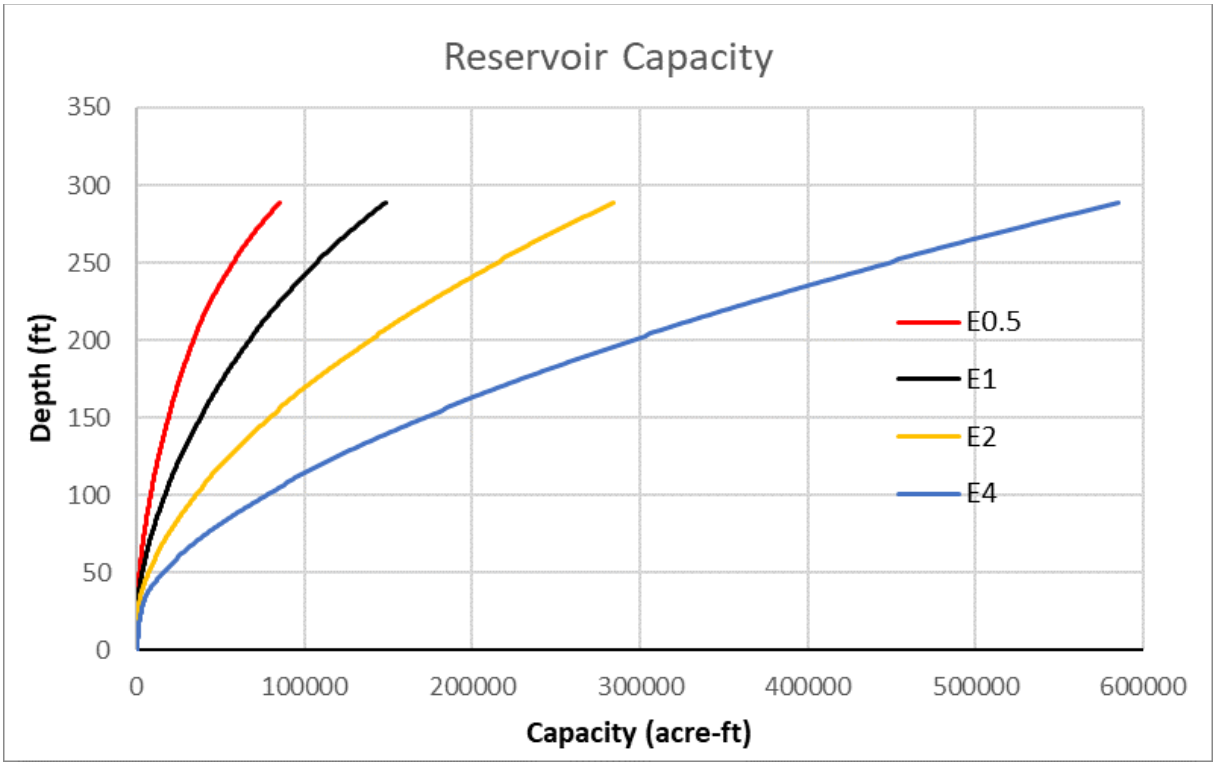

Figure 20.—Reservoir depth vs. capacity with adjusted width.

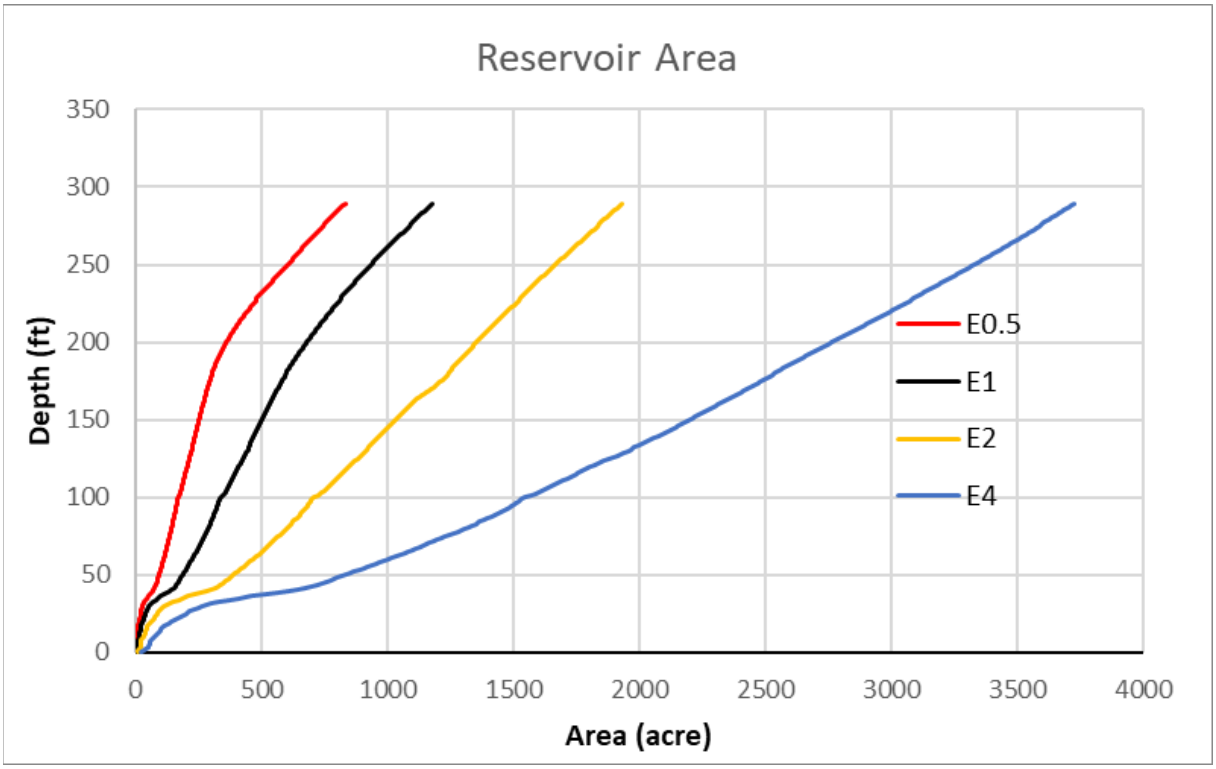

Figure 21.—Reservoir depth vs. area with adjusted width.

Figures 22 through 25 display the new reservoir surface with adjusted width.

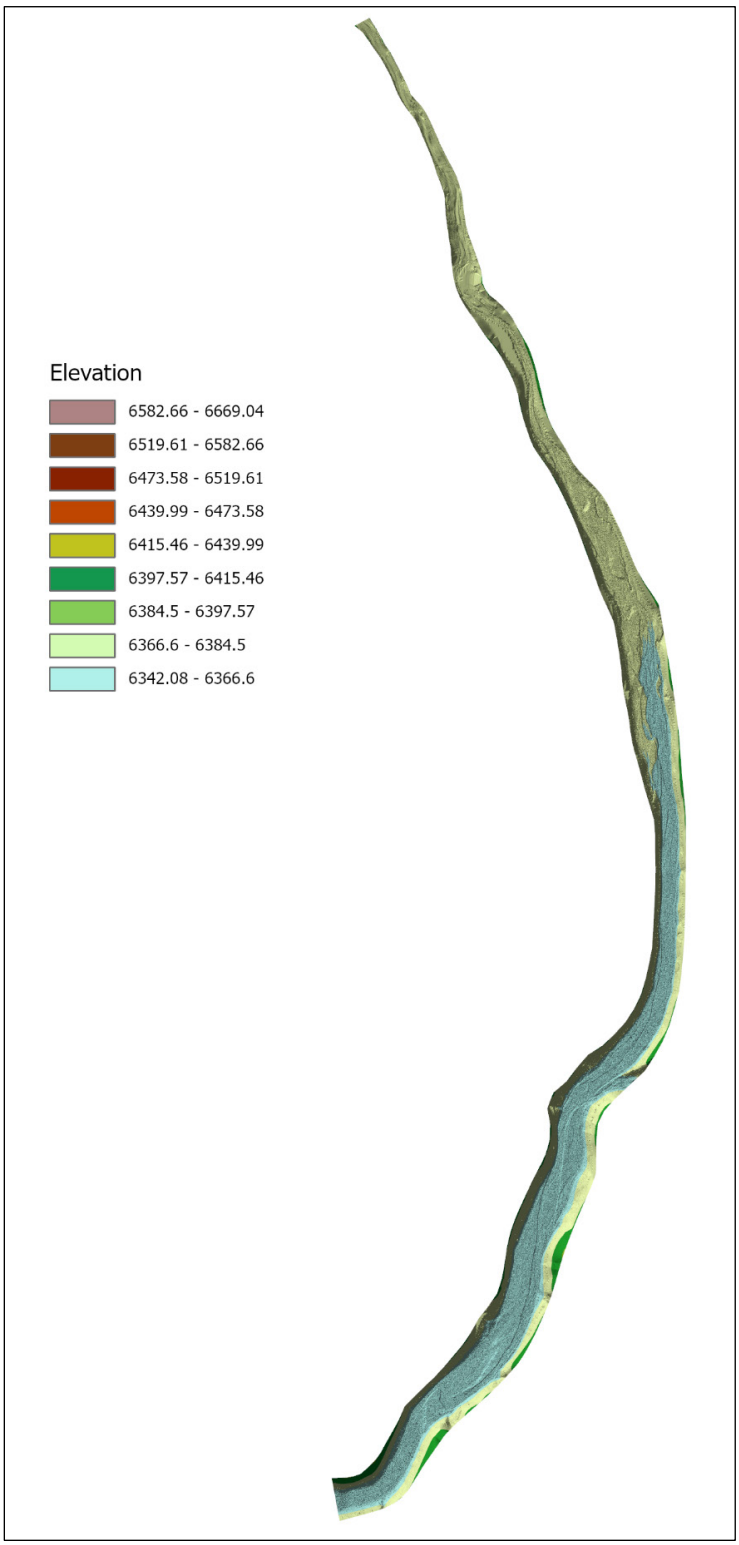

Figure 22.—Paonia Reservoir surface: reduced width (50% of original).

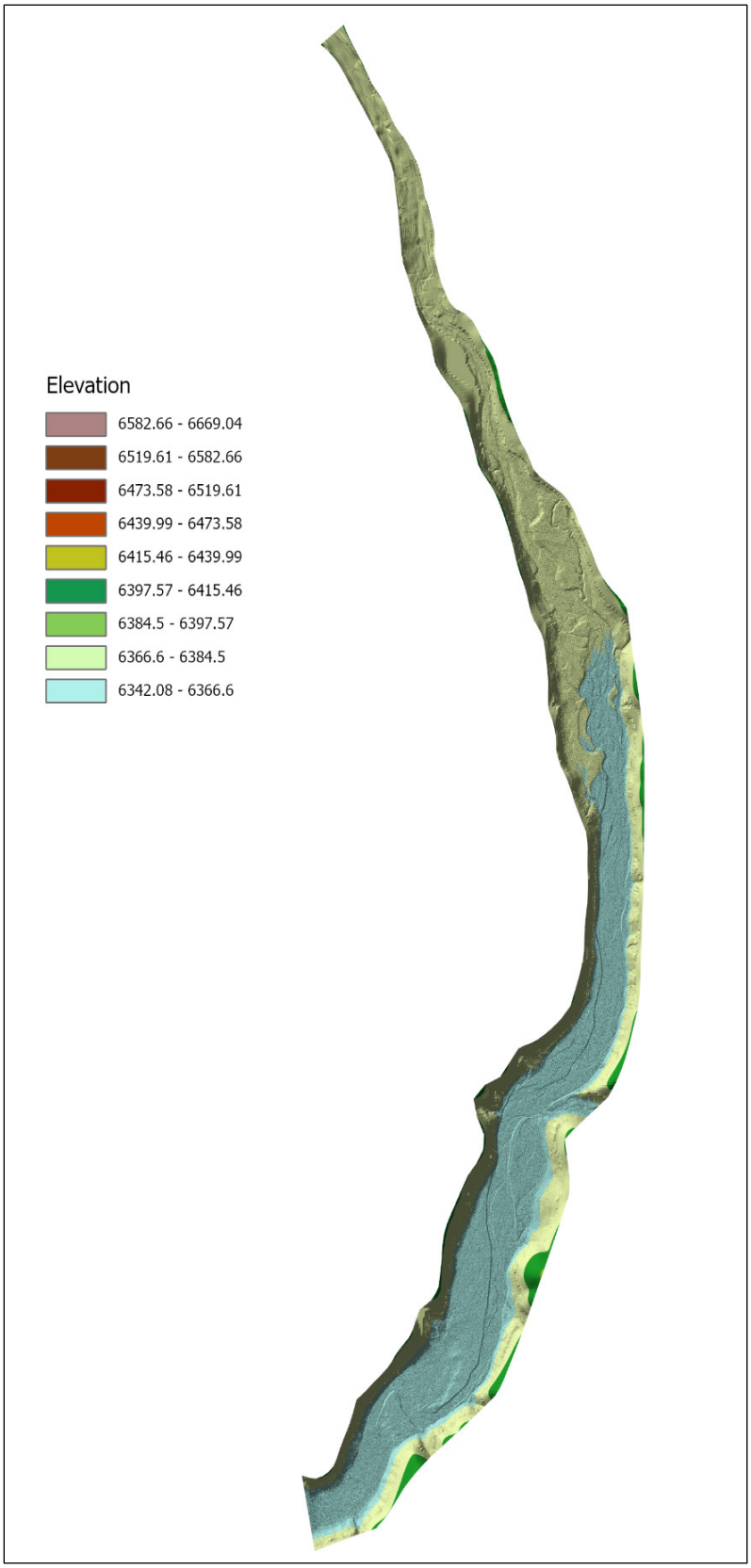

Figure 23.—Paonia Reservoir surface: original width.

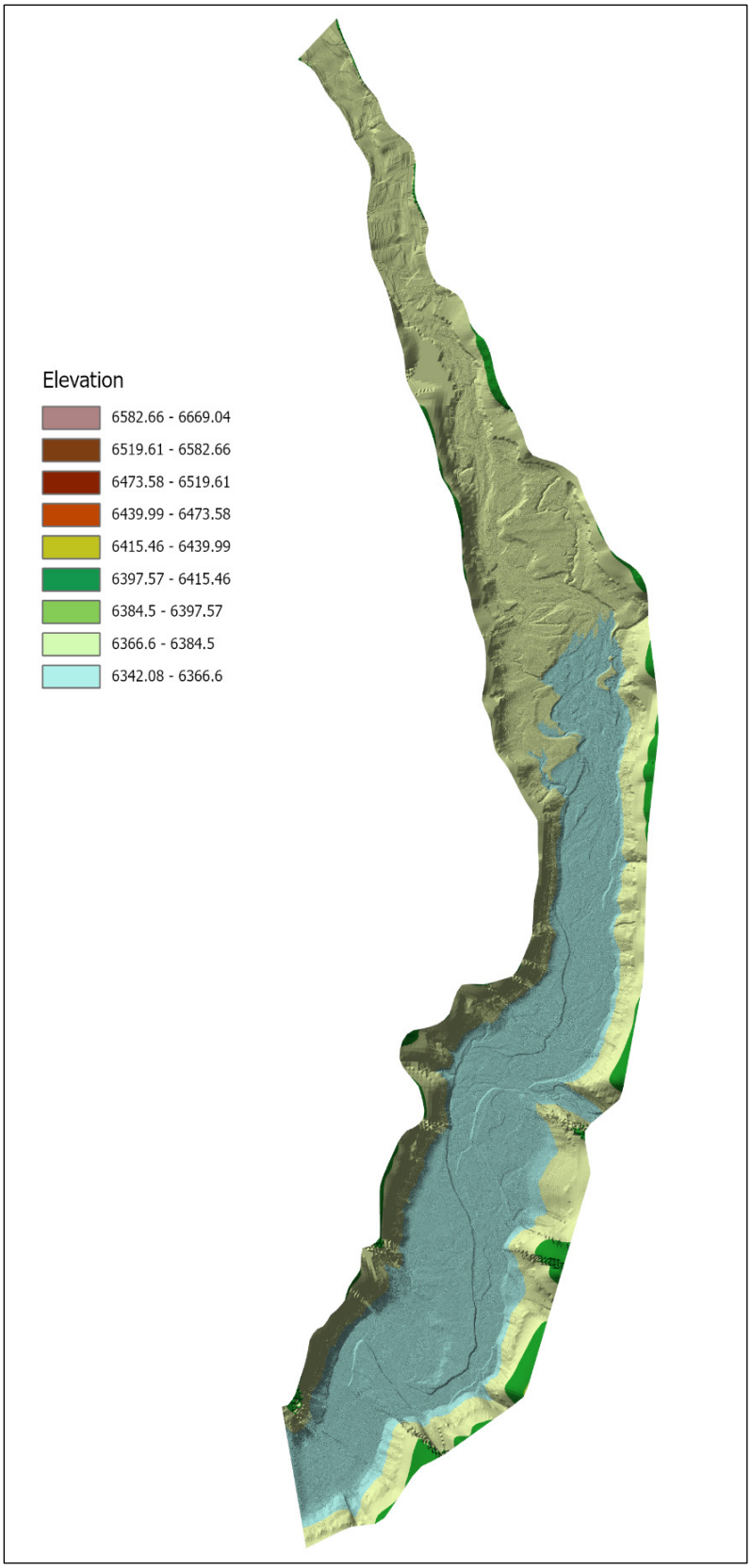

Figure 24.—Paonia Reservoir surface: expended width (2 x original).

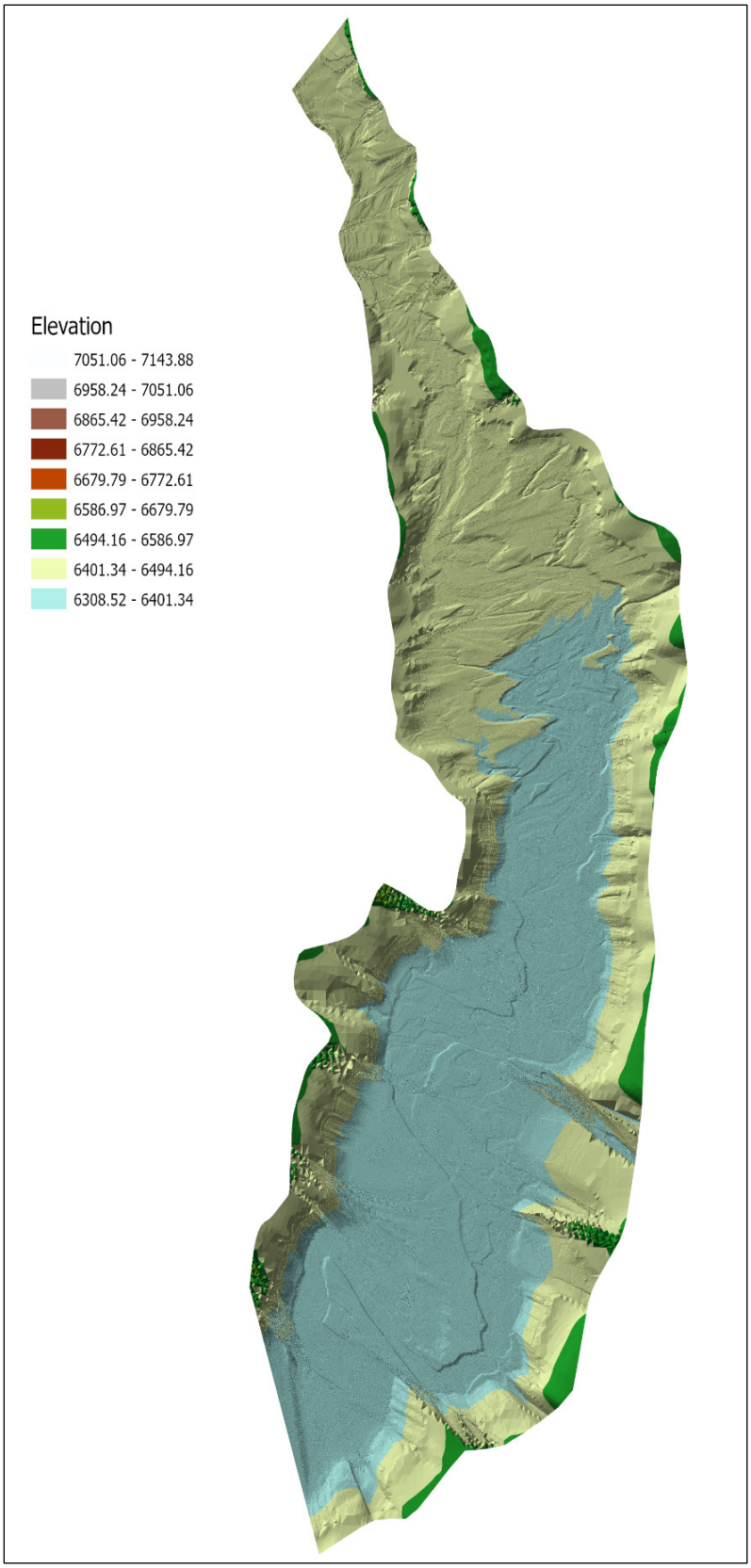

Figure 25.—Paonia Reservoir surface: expended width (4 x original).

6.1. Different Drawdown Flushing Date

To assess the impact of different reservoir drawdown flushing dates on sediment flushing efficiency, various operation rules were implemented. The reservoir was initially maintained at a pool elevation of 6377 ft until February 1. Subsequently, it was drawn down at a rate of one foot per day until reaching 6359 ft, preparing for the spring flushing.

Different flushing ending dates were studied: April 11, April 21, May 1, May 11, May 21, and June 1. Our goal was to determine if prolonged flushing would maintain the same reservoir drawdown flushing efficiency.

Additional reservoir operation rules included restrictions on release flow rates based on pool elevation, reservoir gates of outlet works, and spillway capacity. The reservoir release flow rate should be smaller than the gate capacity of outlet works and greater than the reservoir spillway capacity. The incoming flow rate, reservoir depth-capacity table, and operation rules were used to calculate the pool elevation, as shown in figure 26. The four digital numbers in the figure legend represent the drawdown flushing end date in the format of "mmdd". The pool elevation was be used as downstream boundary condition for the numerical model.

It took approximately 17 days for the reservoir to be filled to a normal pool elevation of 6447.5 ft. For example, with a reservoir drawdown flush end day set at April 11, the reservoir was returned to normal pool elevation on April 28. It was found that with the incoming flow rate of year 2014, if the flushing ended on June 1, there was insufficient incoming flow to refill the reservoir to the normal elevation before the irrigation season began on July 1.

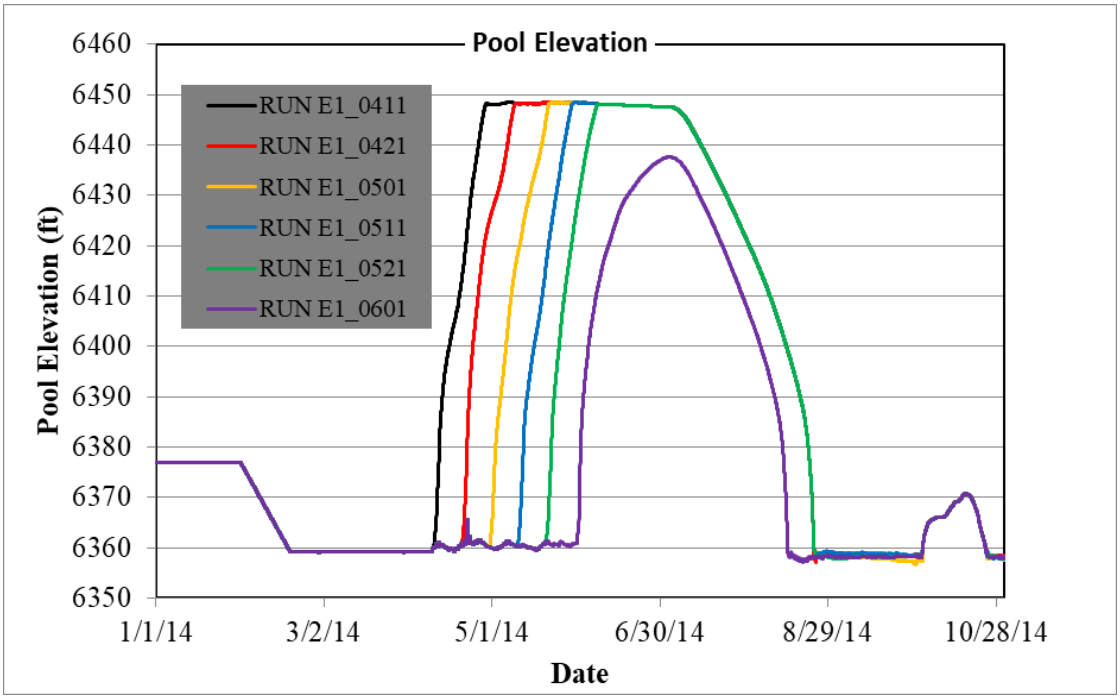

Figure 26.—Reservoir pool elevations with different drawdown flushing dates.

Figure 27 displays the simulated reservoir outflows when the drawdown starts on March 1 and ends on April 21. For better understanding, the reservoir pool elevation is also shown in the same figure. During the drawdown flush period, the reservoir flushing was typically set the same rate as the inflow. However, during peak inflows, the outflow might be smaller than the incoming flow due to the capacity of outlet works. During reservoir refilling period (from April 21 to May 8 in this case), the outflow remained low, allowing most of the incoming water to be used to fill the reservoir. There were some brief spikes in outflow during this period, mostly due to discrepancies between the input pool elevation and the simulated pool elevation from the model. Once the pool reached its normal elevation, the outflow was maintained at approximately the same rate as the incoming flow to ensure a constant pool level.

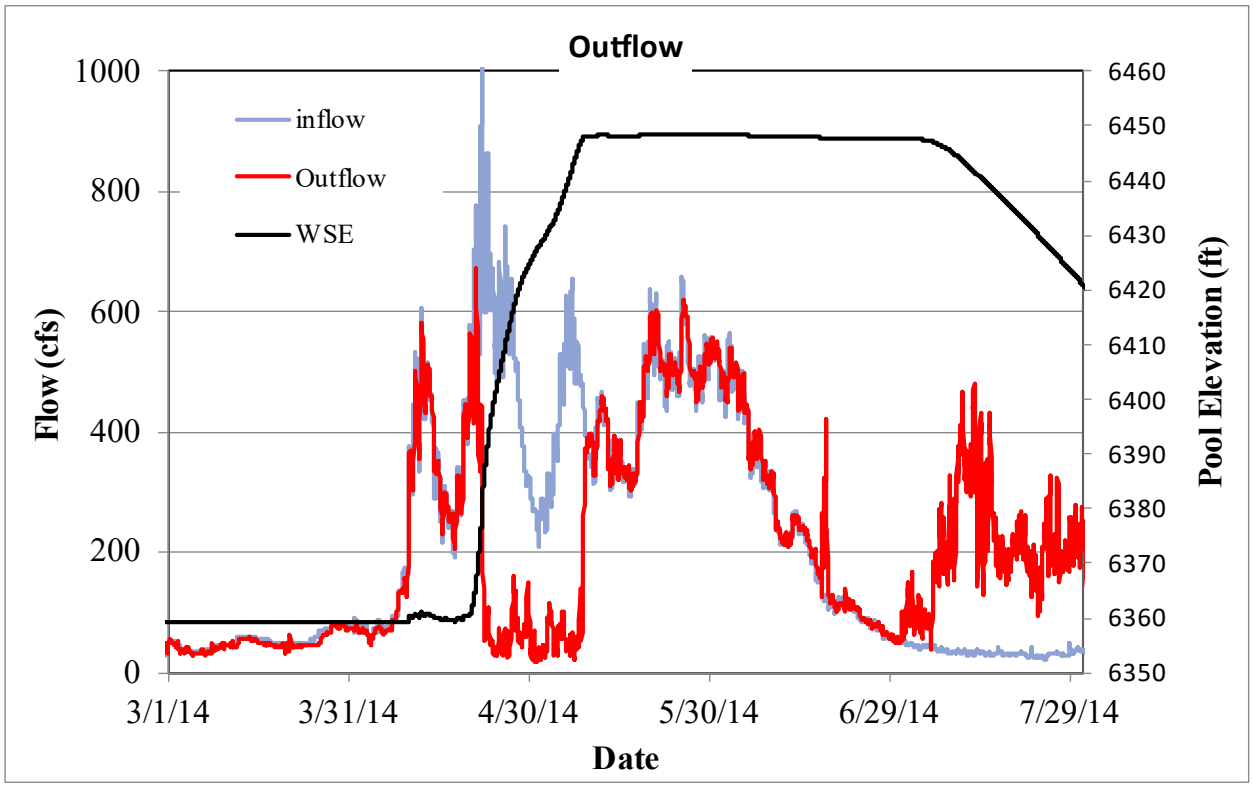

Figure 27.—Simulated reservoir outflow with drawdown flushing end date on April 21.

Figure 28 illustrates the simulated reservoir outflows under different drawdown flushing end dates. When the flushing period was extended, the reservoir outflow was maintained at a higher level to keep the pool elevation lower. This promotes the flushing of more sediment from the reservoir.

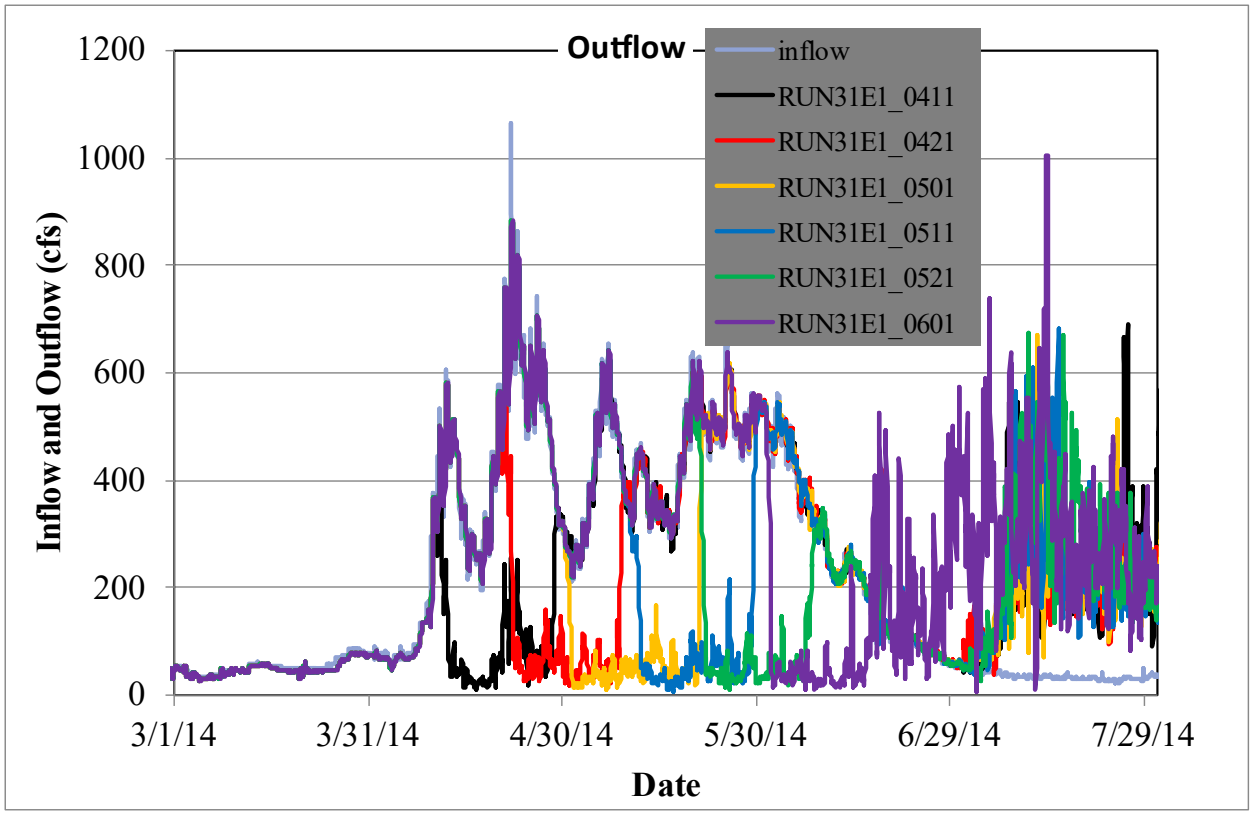

Figure 28.—Simulated reservoir outflows with varying drawdown flushing end dates.

Figure 29 depicts the reservoir release concentration under various drawdown flushing end dates. During the initial period, when incoming flow was low and the reservoir pool elevation was also low, the reservoir release concentration was approximately 1000 mg/L. During the reservoir drawdown flushing period, when the incoming spring flow was high, the sediment release concentration was maintained at a relatively high level, exceeding 10,000 mg/L. During the reservoir filling period, the concentrations decreased significantly to a low level of around 100 mg/L.

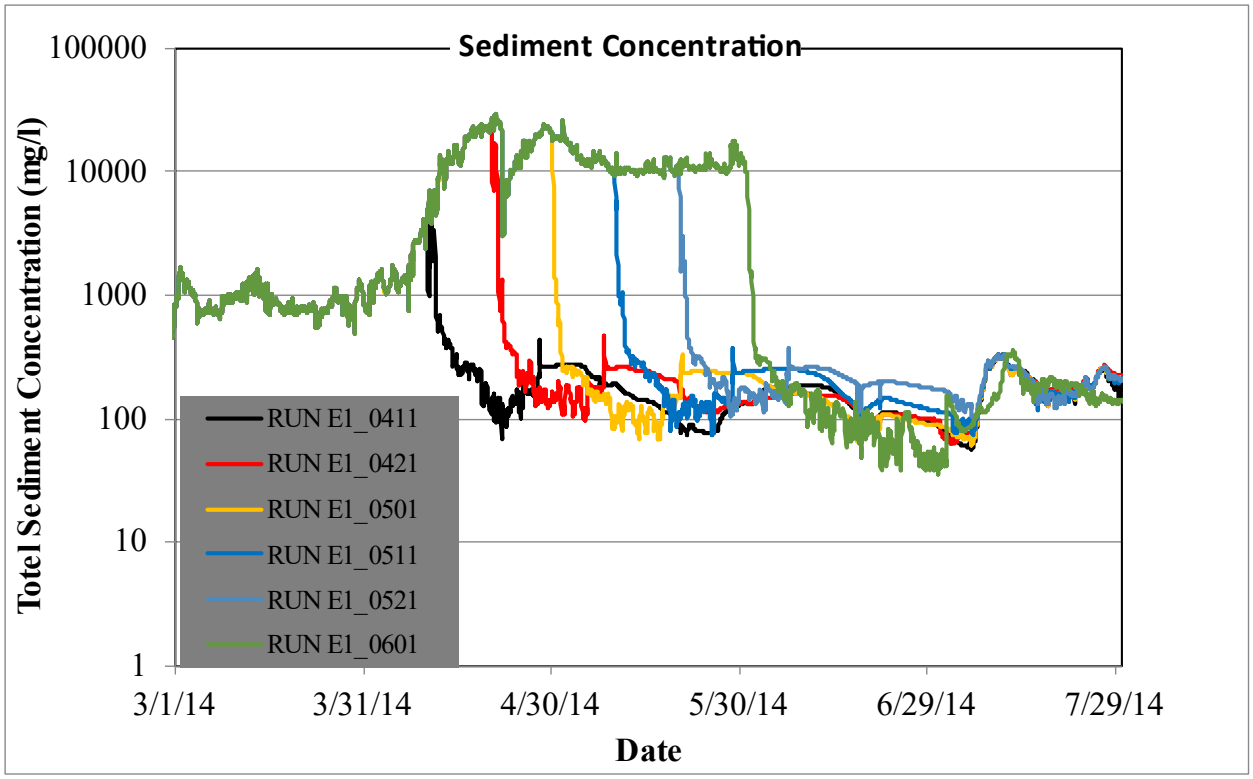

Figure 29.—Simulated reservoir release concentrations with varying drawdown flushing end dates.

Figure 30 presents the sediment load released from the reservoir, comparing it to the incoming sediment load. Numerical results indicate that during the initial flushing period before April 8, nearly all of the incoming sediment was deposited within the reservoir. This suggests that reservoir drawdown flushing is ineffective when the incoming flow is low. Most of the sediment flushing occurred after April 8, when the incoming flow exceeded 350 ft^3/s. During the flushing period, the sediment release load remained relatively constant, resulting in a larger total sediment release with later flushing end dates.

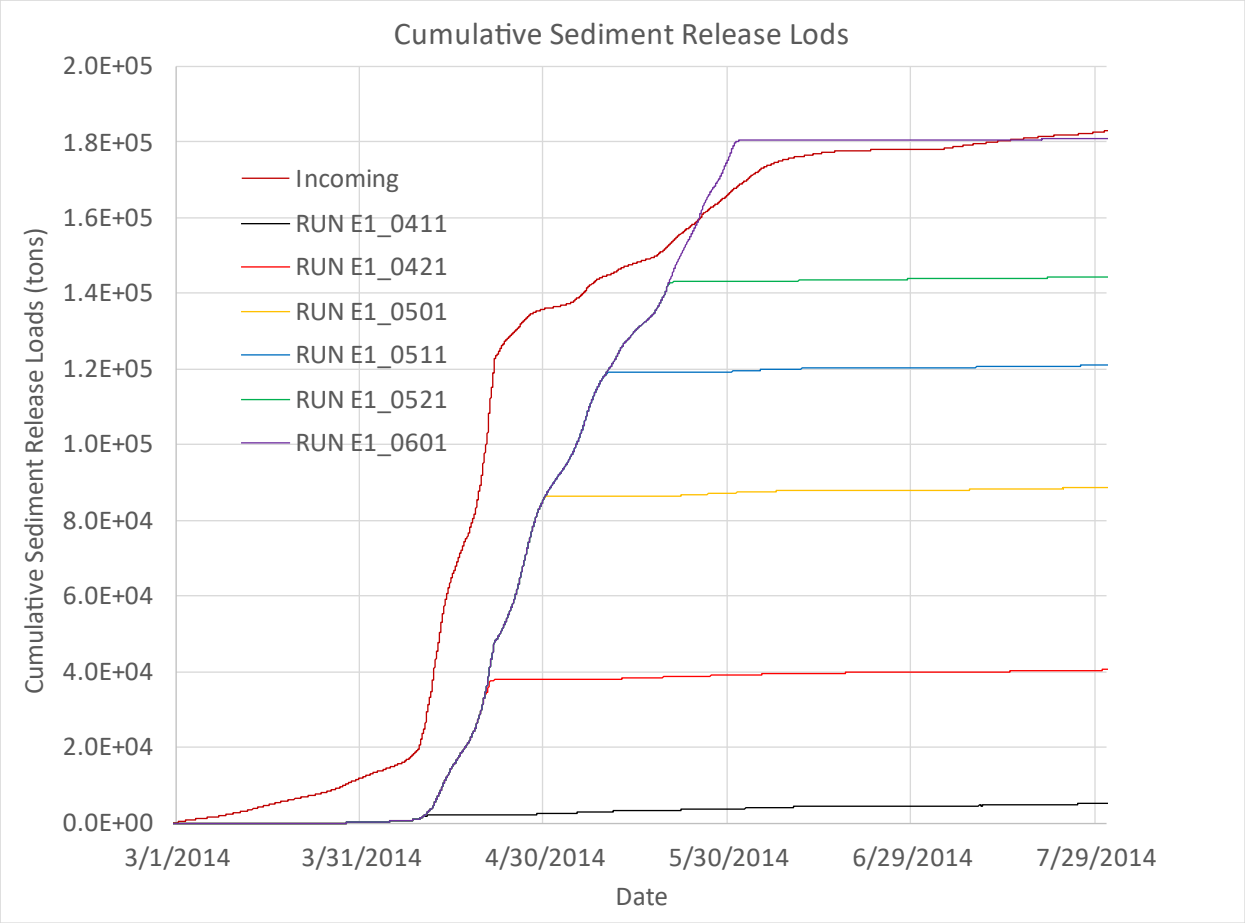

Figure 30.—Impact of flushing end date on cumulative sediment release loads.

Table 5 summarizes the sediment release loads and sediment trapping coefficients for various drawdown flushing end dates. The incoming sediment load is also included for comparison. Model results demonstrate that the flushing end date significantly influences sediment passage through the reservoir. The sediment release load can vary widely, ranging from 4 kilotons (kt) to 180 kt, while the trapping coefficient can be improved from 97% to 1%. It is crucial to extend the drawdown flushing period to maximize sediment removal from the reservoir, provided there is sufficient water to refill the reservoir before the irrigation season begins.

Table 5.—Sediment release loads and reservoir sediment trapping coefficients with varying flushing end dates

Incoming Load (kt)*	**183**					
Flush end date	April 11	April 21	May 1	May 11	May 21	June 1
Release load (kt)	5	40	89	121	144	181
Trapping coefficient	97%	78%	52%	34%	21%	1%

*kt: thousands of English tons

6.2. Comparative Analysis of Reservoir Drawdown Flushing Efficiency in Reservoirs of Varying Widths

Numerical simulations were conducted using identical inflow rates, sedimentation loads, and reservoir operation rules to investigate the influence of reservoir shape on the effectiveness of drawdown flushing. Reservoir shapes were modeled using channel widths that were 0.5, 1, 2, and 4 times the original width of Paonia Reservoir. For this study, the drawdown flushing process was concluded on May 11.

The same reservoir operation rules presented in section 5 were used, which included winter pool elevation, reservoir drawdown before spring flushing, spring flushing, refilling, summer irrigation, reservoir release ramping rate limit, and outlet works and spillway capacities.

As shown in figure 31, the reservoir pool elevation was used as the downstream boundary condition. The numbers in the figure legend represent the ratio of the reservoir width to the original width. The reservoir reached its normal pool elevation of 6447.5 ft in approximately 10 and 17 days, respectively, for reduced reservoir width (50%) and original width (100%). When the reservoir width was doubled, it filled to near the normal elevation but did not fully reach it. With a reservoir width four times the original, the pool elevation only reached 6416 ft, which is about 31 ft lower than normal.

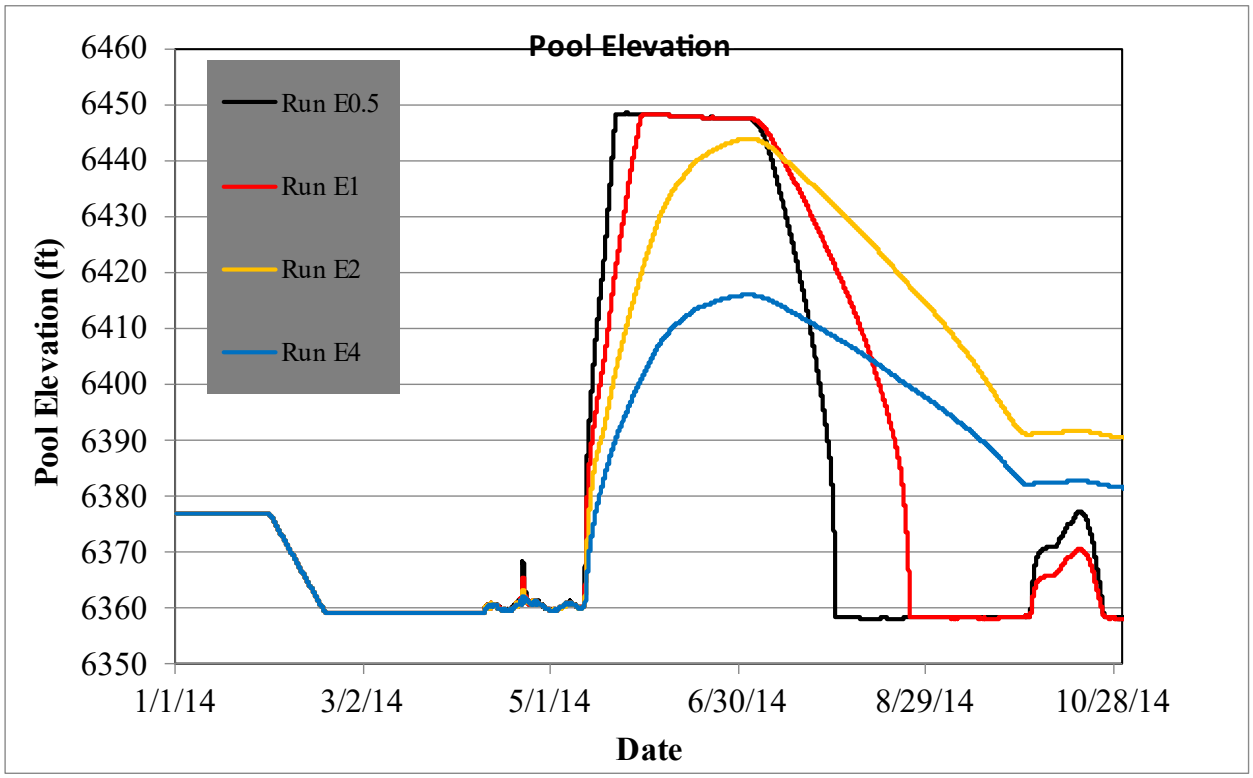

Figure 31.—Reservoir pool elevations with different reservoir widths.

Figure 32 illustrates the simulated reservoir outflows for four different reservoir widths, assuming a drawdown period from March 1 to May 11. For comparison, the incoming flow rate is also depicted in the same figure.

It is puzzling that, in Run E4, the outflow was calculated to be nearly zero before April 8, the date the spring flood entered reservoir. It was expected that low incoming flow period would not impact the calculation of the sediment loads flushed out of the reservoir during the spring flood.

The peak outflow during the flushing period was lower than the incoming flow due to the limitations of the outlet works.

After May 11, the end of the flushing period, the reservoir outflow remained at a low level until the reservoir was full. The reservoir filling time was extended for reservoirs with larger widths and capacities.

The results also indicate that there are numerous spikes in the reservoir filling period and summer irrigation period for reservoirs with widths 2 and 4 times the original. This may be attributed to the use of a preset pool elevation as a downstream boundary condition, which was calculated based on the current depth and capacity table without considering potential capacity changes during the simulation. Further research is needed to determine the exact cause of these spikes.

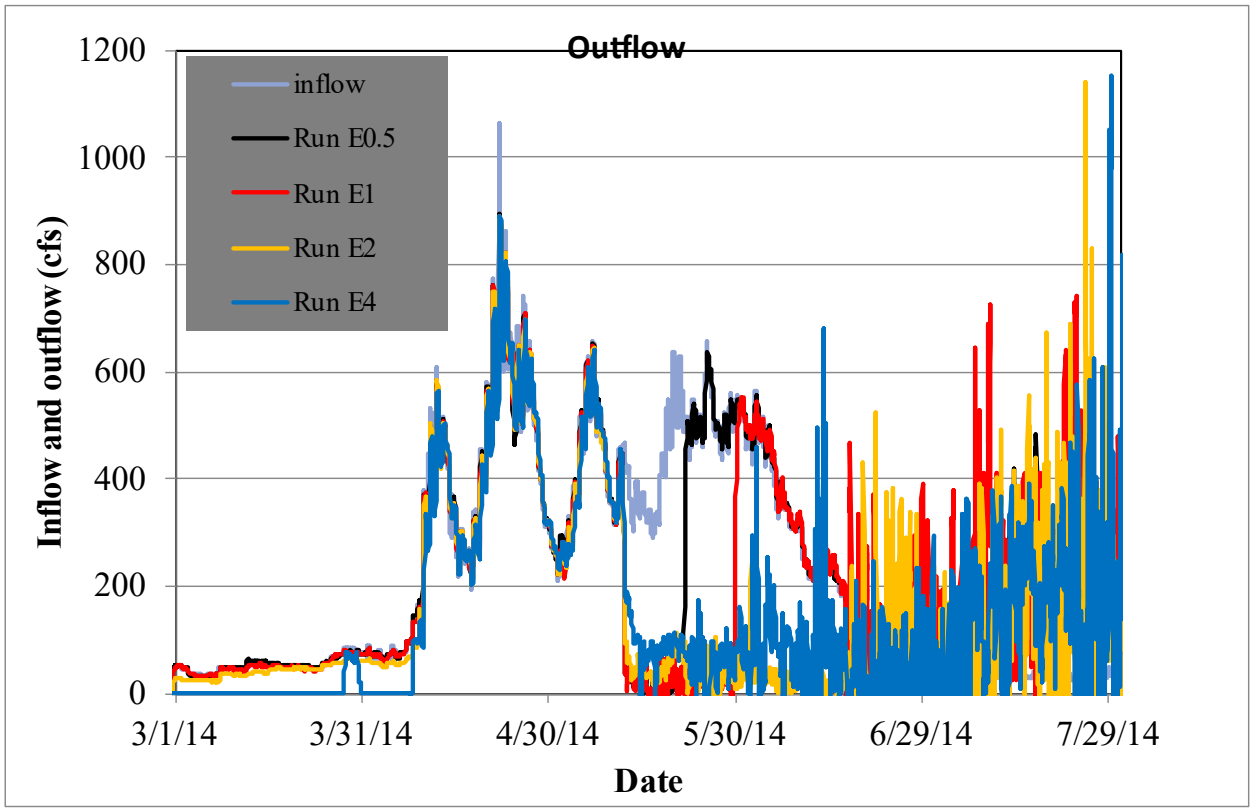

Figure 32.—Reservoir release with different reservoir widths.

Figure 33 presents the concentration of sediment released from the reservoir for various reservoir widths. High sediment concentrations in the reservoir release occurred during the spring flood season, coinciding with the reservoir drawdown period from April 8 to May 11. The reservoir release concentration decreases as the reservoir width increases.

However, when comparing reservoirs with widths 2 and 4 times the original, a curious phenomenon was observed. During the drawdown flushing period, the sediment concentrations are nearly identical. This suggests that expanding the reservoir's width beyond a certain point may not reduce flushing efficiency. A possible explanation lies in the formation of a narrow pilot channel during drawdown flushing which improves the effectiveness of the flushing.

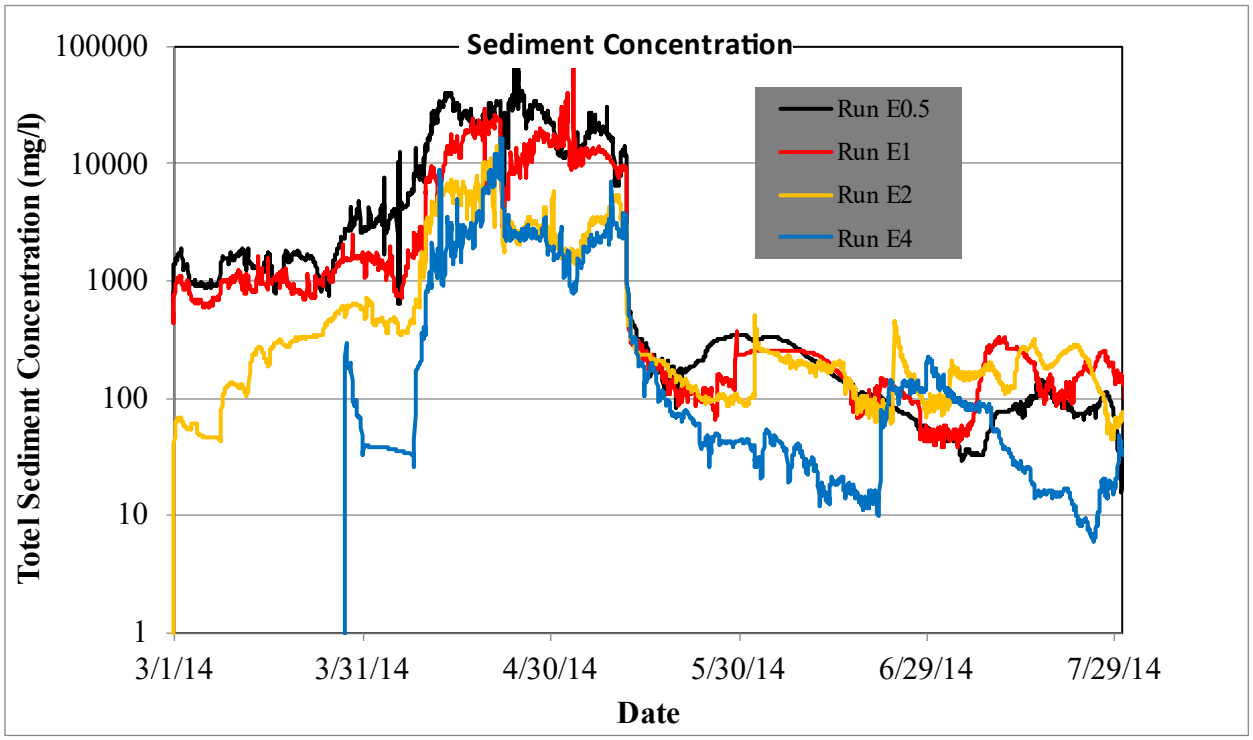

Figure 33.—Reservoir release concentration with different reservoir widths.

Figure 34 compares the sediment load released from the reservoir to the incoming sediment load. The majority of sediment releases occurred during the spring flood period, coinciding with the drawdown flushing from April 8 to May 11. Prior to the spring flood, there were virtually no noticeable sediment releases, even when the reservoir pool was low.

A smaller reservoir width was found to be more efficient in passing sediment downstream during the flushing process. However, continued increase in the width did not significantly reduce the sediment release load.

This intriguing phenomenon suggests that sediment drawdown flushing could be a viable option for reservoirs with wider widths. By understanding the formation of pilot channels and their impact on flushing efficiency, reservoir managers can explore strategies to optimize sediment removal, even in larger reservoirs.

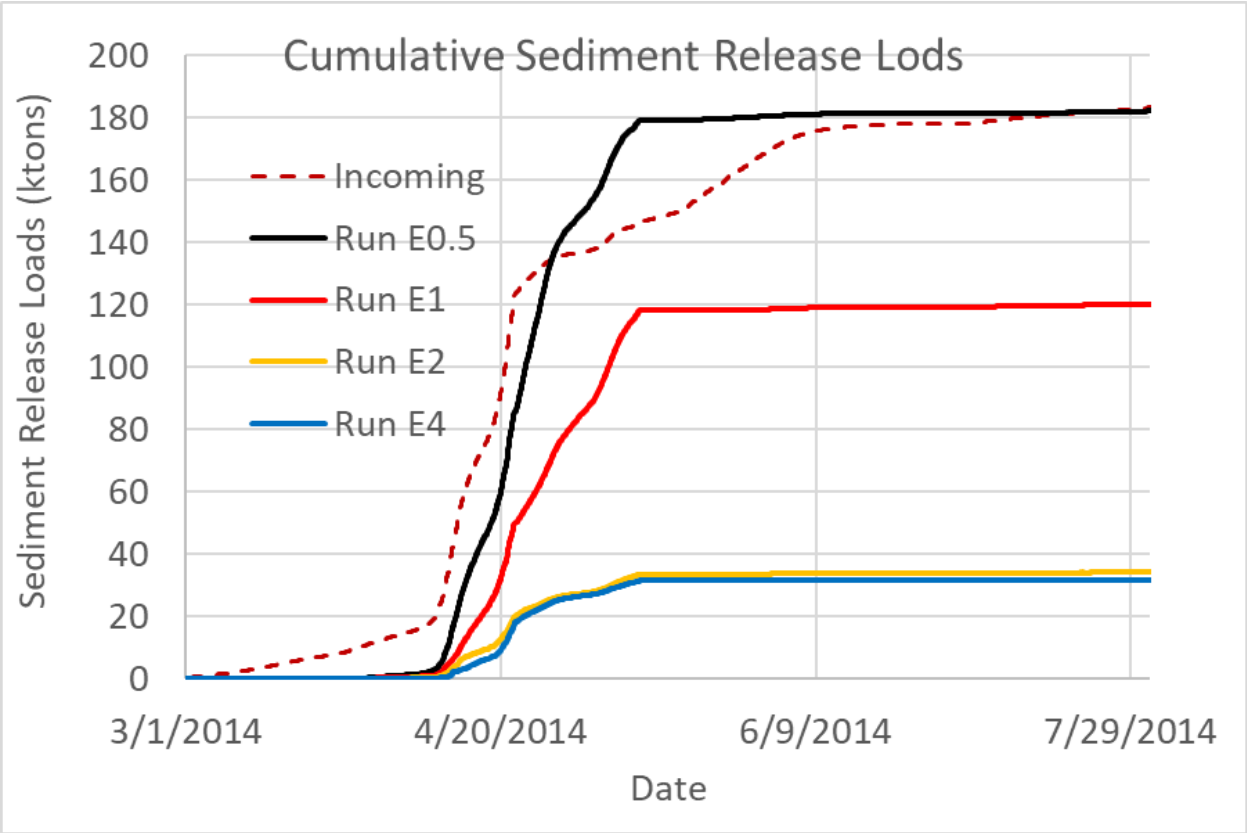

Figure 34.—Reservoir release loads with different reservoir widths.

Table 6 summarizes the sediment release loads and sediment trapping coefficients for reservoirs of various widths and capacities. The trapping coefficients range from 1% for a Type IV reservoir with a very narrow bottom, to 83% for a Type I reservoir with a much wider bottom.

Table 6.—Sediment release loads and reservoir sediment trapping coefficients with varying flushing end dates

Incoming load (kt)*	**183**			
Run	Run E0.5	Run E1	Run E2	Run E4
Release load (kt)	182	120	34	32
Trapping coefficient	1%	34%	81%	83%

*kt: thousands of English tons

7.0 Summary

A literature review of numerical modeling studies on reservoir drawdown flushing was conducted, encompassing 1D, 2D, and 3D models. General concepts for reservoir drawdown flushing have also been summarized in this report.

The SRH-2D model was used to simulate spring flushing conducted at the Paonia Reservoir in 2014, using available field data for calibration. The model was calibrated to accurately reproduce sediment release concentrations and loads during the drawdown flushing event. Calibration parameters included sediment layer thickness and cohesive sediment transport parameters such as critical shear stresses for deposition, surface erosion, mass erosion, and fall velocity.

Various reservoir shapes were created to investigate their effects on reservoir drawdown flushing efficiency. Two approaches were employed to modify reservoir shapes: 1) altering reservoir width at different depths while maintaining a fixed reservoir capacity at normal depth while, and 2) modifying the width to ratios of 0.5, 1, 2, and 4 times the original width, with corresponding adjustments to reservoir capacity.

Reservoir operation rules, including winter pool elevation, drawdown flushing elevation, refilling date, and summer irrigation flow rate, were implemented to determine reservoir pool elevations during the simulation period. Combined with the reservoir capacity table at different pool elevation, the reservoir pool elevations were established in advance to serve as downstream boundary conditions for the simulations.

Results indicated that when maintaining constant reservoir capacity, Type IV reservoirs (narrower at the bottom) achieved the highest sediment flushing efficiency, while Type I reservoirs (wider at the bottom) exhibited the lowest efficiency. Trapping coefficients ranged from 34% for Type I to 15% for Type IV during the period from March 1 to August 1.

When reservoir capacity was varied, narrow reservoirs with reduced capacities displayed superior sediment flushing efficiency. Based on the Paonia Reservoir, the sediment trapping coefficient ranged from 1% for a reservoir half the original size to 83% for a one four times its width. However, beyond a certain limit, increasing reservoir width did not significantly increase the trapping coefficient, indicating that drawdown flushing remains a degree of effectiveness for even wider reservoirs.

To optimize sediment removal from the reservoir, it is essential to extend the duration of drawdown flushing, provided there is adequate water available for refilling before the onset of the irrigation season.

8.0 References

Ackers, P., and Thompson, G. (1987). "Reservoir sedimentation and influence of flushing." Sediment Transport in Gravel-Bed Rivers. John Wiley and Sons New York. 1987. p 845–868, 5 fig, 13 ref.

Ahn, J. (2012). "Numerical modeling of reservoir sedimentation and flushing processes." Colorado State University.

Ahn, J., Yang, C.T., Pridal, D.B., and Remus, J.I. (2013). "Numerical modeling of sediment flushing from Lewis and Clark Lake." *International Journal of Sediment Research*, Elsevier, 28(2), 182–193.

Annandale, G.W. (1987). "Developments in Water Science- Reservoir Sedimentation." BV Rand Afrikaans University: Elsevier Science Publishers.

Annandale, G.W. (2001). "Reservoir conservation and sediment management." *Water week*.

Artruc, T.C. (2020). "Numerical Modeling of Lateral Erosion during Reservoir Drawdown."

Atkinson, E. (1996). "The feasibility of flushing sediment from reservoirs." HR Wallingford Ltd.

Basson, G. R. (2009). "Management of siltation in existing and new reservoirs. General Report." The 23rd Congress of the International Commission on Large Dams, Int. Com. on Large Dams, Brasilia.

Boeriu, P., Roelvink, D., Mulatu, C.A., Thilakasiri, C.N., Moldovanu, A., and Margaritescu, M. (2011). "Modeling the flushing process of reservoirs." *The Romanian Review Precision Mechanics*, (40), 54.

Borland, W. and Miller, C. (1960). Distribution of sediment in large reservoirs. Transactions of the American Society of Civil Engineers, 125(1), 166–180.

Boyd, P.M., and Gibson, S.A. (2016). "Applying 1d sediment models to reservoir flushing studies: measuring, monitoring, and modeling the spencer dam sediment flush with HEC-RAS." Coastal and Hydraulics Laboratory (U.S.).

Brignoli, M.L. (2017). "Improving sustainability of sediment management in Alpine reservoirs: control of sediment flushing operations to mitigate downstream environmental impacts." Università degli Studi dell'Insubria.

Chang, H.H., Harrison, L.L., Lee, W., and Tu, S. (1996). "Numerical modeling for sediment-pass-through reservoirs." *Journal of Hydraulic Engineering*, American Society of Civil Engineers, 122(7), 381–388.

Chaudhary, H.P., Isaac, N., Tayade, S.B., and Bhosekar, V.V. (2019). "Integrated 1D and 2D numerical model simulations for flushing of sediment from reservoirs." *ISH Journal of Hydraulic Engineering*, Taylor and Francis, 25(1), 19–27.

Chen, C.-N., and Tsai, C.-H. (2017). "Estimating sediment flushing efficiency of a shaft spillway pipe and bed evolution in a reservoir." *Water*, Multidisciplinary Digital Publishing Institute, 9(12), 924.

Dahl, T. A., and Ramos-Villanueva, M. (2019). "Overview of historical reservoir flushing events and screening guidance." Coastal and Hydraulics Laboratory (U.S.).

Dewals, B., Erpicum, S., Archambeau, P., Detrembleur, S., Fraikin, C., and Pirotton, M. (2004). "Large scale 2D numerical modelling of reservoirs sedimentation and flushing operations." *Proceedings of the 9th International Symposium on River Sedimentation*.

Esmaeili, T., Sumi, T., Kantoush, S. A., Kubota, Y., and Haun, S. (2015). "Numerical study on flushing channel evolution, case study of Dashidaira reservoir, Kurobe river." *土木学会論文集 B1 (水工学)*, 公益社団法人 土木学会, 71(4), I_115-I_120.

Esmaeili, T., Sumi, T., Kantoush, S.A., Kubota, Y., Haun, S., and Rüther, N. (2017). "Three-dimensional numerical study of free-flow sediment flushing to increase the flushing efficiency: a case-study reservoir in Japan." *Water*, Multidisciplinary Digital Publishing Institute, 9(11), 900.

Ghoreishi, S. H., and Tabatabai, M.M.R. (2010). "Model study reservoir flushing." *Journal of Water Sciences Research* (JWSR), 2(1), 1–8.

Goulart, C. B., Bleninger, T., de Oliveira Fagundes, H., and Fan, F. M. (2023). Modeling uncertainties of reservoir flushing simulations. International Journal of Sediment Research, 38(5), 698-710.

Guertault, L., Camenen, B., Paquier, A., and Peteuil, C. (2014). "1D Modelling of fine sediments dynamics in a dam reservoir during a flushing event." *Proceedings of 7th International Conference on Fluvial Hydraulics, Lausanne, Switzerland*, CRC Press, Lausanne, Switzerland, 147–154.

Haun, S., and Olsen, N.R.B. (2012). "Three-dimensional numerical modelling of the flushing process of the Kali Gandaki hydropower reservoir." *Lakes & Reservoirs: Research & Management*, Wiley Online Library, 17(1), 25–33.

Huang, J., Greimann, B., and Kimbrel, S. (2019). "Simulation of Sediment Flushing in Paonia Reservoir of Colorado." *Journal of Hydraulic Engineering*, 145(12).

Iqbal, M., Ghumman, A.R., Haider, S., Hashmi, H.N., and Khan, M.A. (2019). "Application of Godunov type 2D model for simulating sediment flushing in a reservoir." *Arabian Journal for Science and Engineering*, Springer, 44(5), 4289–4307.

Kimbrel, S. (2015). Numerical Modeling and Analysis of Sediment Transport at Paonia Reservoir: SRH-1D Model Calibration and 2015 Operations. Report SRH-2015-32, Sedimentation and River Hydraulics Group, Technical Service Center, Bureau of Reclamation, Denver, CO.

Kondolf, G. M., Gao, Y., Annandale, G. W., Morris, G. L., Jiang, E., Zhang, J., Cao, Y., Carling, P., Fu, K., and Guo, Q. (2014). "Sustainable sediment management in reservoirs and regulated rivers: Experiences from five continents." *Earth's Future*, Wiley Online Library, 2(5), 256–280.

Lai, Y. G. (2020). SRH-2D User's Manual: Sediment Transport and Mobile-Bed Modeling. Sedimentation and River Hydraulic Group. Technical Service Center, Bureau of Reclamation, Denver.

Lai, J.-S., and Shen, H.W. (1996). "Flushing sediment through reservoirs." *Journal of Hydraulic Research*, Taylor and Francis, 34(2), 237–255.

Lai, J.S., and Shen, H. W. (1995). "An experiment study on reservoir drawdown flushing." *International Journal of Sediment Research*, 10(3), 19–36.

Lai, Y.G., and Greimann, B.P. (2012). "Modeling channel formation on the Klamath River due to reservoir drawdown." *United States Society of Dams Annual Meeting and Conference*, New Orleans, Louisiana.

Lai, Y. G., Huang, J., and Greimann, B. P. (2024). Hydraulic Flushing of Sediment in Reservoirs: Best Practices of Numerical Modeling. Fluids , 9(2), 38.

Liu, J., Minami, S., Otsuki, H., Liu, B., and Ashida, K. (2004). "Prediction of concerted sediment flushing." *Journal of Hydraulic Engineering*, American Society of Civil Engineers, 130(11), 1089–1096.

Mahmood, K. (1987). Reservoir sedimentation: impact, extent, and mitigation. Technical paper. International Bank for Reconstruction and Development, Washington, D.C. (USA).

Minami, S., Noguchi, K., Otsuki, H., Fukuri, H., Shimahara, N., Mizuta, J., and Takeuchi, M. (2012). "Coordinated sediment flushing and effect verification of fine sediment discharge operation in Kurobe River." Proceedings of the ICOLD Conference, Kyoto, Japan, 6–8.

Morris, G. L., and Fan, J. (1998). *Reservoir sedimentation handbook: design and management of*

dams, reservoirs, and watersheds for sustainable use. McGraw Hill Professional.

Morris, G. L., and Hu, G. (1992). "HEC-6 modeling of sediment management in Loíza Reservoir, Puerto Rico." Hydraulic Engineering: Saving a Threatened Resource—In Search of Solutions, ASCE, 630–635.

Olsen, N. R. B. (1999). "Two-dimensional numerical modelling of flushing processes in water reservoirs." *Journal of Hydraulic research*, Taylor and Francis, 37(1), 3–16.

Olsen, N. R. B., and Haun, S. (2018). "Numerical modelling of bank failures during reservoir draw-down." EDP Sciences.

Randle, T.J., Bountry, J.A., Ritchie, A., and Wille, K. (2015a). "Large-scale dam removal on the Elwha River, Washington, USA: Erosion of reservoir sediment." *Geomorphology*, Elsevier, 246, 709–728.

Randle, T.J., Kimbrel, S., and Collins, K.L. (2015b). "Reservoir sustainability workshop and national reservoir sedimentation team." *The 3rd Joint Federal Interagency Conference*, (figure 4), 1–11.

Saam, L., Mouris, K., Wieprecht, S., and Haun, S. (2019). "Three-dimensional numerical modelling of reservoir flushing to obtain long-term sediment equilibrium." *Proceedings of the 38th IAHR World Congress, Panama City, Panama*, 1–6.

Shen, H.W. (1999). "Flushing sediment through reservoirs." *Journal of Hydraulic Research*, Taylor and Francis, 37(6), 743–757.

Sumi, T. (2008). "Evalutation of Efficienca of Reservoir Sediment Flushing in Kurobe River." *Proceedings 4th International Conference on Scour and Erosion (ICSE-4).* November 5–7, 2008, Tokyo, Japan, 608–613.

Talebbeydokhti, N., and Naghshineh, A. (2004). "Flushing sediment through reservoirs." *Iranian Journal of Science and Technology, Transaction B: Engineering*, Taylor and Francis, 28(B1), 119–136.

White, R. (2001). Evacuation of sediments from reservoirs. Thomas Telford.

White, W.R. (1990). "Reservoir sedimentation and flushing." *Hydrology in Mountainous Regions. Artificial Reservoirs; Water and Slopes. IAHS Publ*, (194).

Wisser, D., Frolking, S., Hagen, S., and Bierkens, M. F. P. (2013). "Beyond peak reservoir storage? A global estimate of declining water storage capacity in large reservoirs." *Water Resources Research*, Wiley Online Library, 49(9), 5732–5739.